Evaluation of land surface model simulations of evapotranspiration over a 12-year crop succession: impact of soil hydraulic and vegetation properties.

Garrigues, Sébastien[1,2]; Olioso Albert[1,2]; Calvet, Jean-Christophe[3]; Martin, Eric[3]; Lafont, Sébastien[5] ; Moulin, Sophie[1,2]; Chanzy, André [1,2]; Marloie, Olivier[4]; Desfonds, Véronique[1,2]; Bertrand, Nadine[1,2]; Renard, Dominique[1,2], Buis, Samuel[1,2].

[1] INRA, UMR1114 EMMAH, F-84914 Avignon Cedex 9, France

[2] Université d'Avignon et des Pays de Vaucluse, UMR1114 EMMAH, F-84000 Avignon, France

[3] CNRM-GAME, UMR3589, Météo-France, CNRS, Toulouse, France

[4] URFM, INRA, Avignon, France

[5] ISPA, INRA, Bordeaux, France

Submitted to Hydrology and Earth System Sciences

Abstract

Evapotranspiration has been recognized as one of the most uncertain term in the surface water balance simulated by land surface models. In this study, the SURFEX/ISBA-A-gs simulations of evapotranspiration are assessed at the field scale over a 12-year Mediterranean crop succession. The model is evaluated in its standard implementation which relies on the use of the ISBA pedotransfer estimates of the soil properties. The originality of this work consists in explicitly representing the succession of crop cycles and inter-crop bare soil periods in the simulations and assessing its impact on the dynamics of simulated and measured evapotranspiration over a long period of time. The analysis focuses on key parameters which drive the simulation of ET, namely the rooting depth, the soil moisture at saturation, the soil moisture at field capacity and the soil moisture at wilting point. A sensitivity analysis is first conducted to quantify the relative contribution of each parameter on ET simulation over 12 years. The impact of the estimation method used to retrieve the soil parameters (pedotransfer function, laboratory and field methods) on ET is then analyzed. The benefit of representing the variations in time of the rooting depth and wilting point is evaluated. Finally, the propagation of uncertainties in the soil parameters on ET simulations is quantified through a Monte-Carlo analysis and compared with the uncertainties triggered by the mesophyll conductance which is a key above-ground driver of the stomatal conductance.

This work shows that evapotranspiration mainly results from the soil evaporation when it is continuously simulated over a Mediterranean crop succession. This results in a high sensitivity of simulated evapotranspiration to uncertainties in the soil moisture at field capacity and the soil moisture at saturation which both drive the simulation of soil evaporation. Field capacity was proved to be the most influencing parameter on the simulation of evapotranspiration over the crop succession. The evapotranspiration simulated with the standard surface and soil parameters of the model is largely underestimated. The deficit in cumulative evapotranspiration amounts to 24% over 12 years. The bias in daily daytime evapotranspiration is -0.24 mm day^{-1}. The ISBA pedotransfer estimates of the soil moisture at saturation and at wilting point are overestimated which explains most of the evapotranspiration underestimation. The use of field capacity values retrieved from laboratory methods leads to inaccurate simulation of ET due to the lack of representativeness of the soil structure variability at the field scale. The most accurate simulation is achieved

with the average values of the soil properties derived from the analysis of field measurements of soil moisture vertical profiles over each crop cycle. The representation of the variations in time of the wilting point and the maximum rooting depth over the crop succession has little impact on the simulation performances. Finally, we show that the uncertainties in the soil parameters can generate substantial uncertainties in ET simulated over 12 years (the 95% confidence interval represents 23% of cumulative ET over 12-years). Uncertainties in the mesophyll conductance have lower impact on ET. Measurement random errors explain a large part of the scattering between simulations and measurements at half-hourly time scale. The deficits in simulated ET reported in this work are probably larger due to likely underestimation of ET by eddy-covariance measurements. Other possible model shortcomings include the lack of representation of soil vertical heterogeneity and root profile along with inaccurate energy balance partitioning between the soil and the vegetation at low LAI.

Keys words:

Land surface model, evapotranspiration, crop succession, soil hydraulic properties, eddy covariance.

1 Introduction

Land surface models (LSMs) are relevant tools to analyze and predict the evolution of the water balance at various spatial and temporal scales. They describe water, carbon and energy fluxes between the surface and the atmosphere at hourly time scale. Most LSMs consist of 1-D column models describing the non-saturated soil (mainly the root-zone), the vegetation and the surface/atmosphere interaction processes. The LSM complexity mainly differs in 1) the number of sources involved in the surface energy balance, 2) the representation of water and thermal soil transfers, 3) the representation of stomatal conductance (see reviews in Olioso et al., 1999; Arora, 2002; Pitman, 2003; Overgaard et al., 2006; Bonan, 2010). For example, the original version of the Interactions between Soil, Biosphere, and Atmosphere (ISBA, Noilhan and Planton (1989)) computes a single energy budget assuming an unique "big leaf" layer. It is a simple bucket model based on the force-restore method with two or three soil layers. The stomatal conductance is simply represented by the Jarvis, (1976) empirical formulation. More advanced LSMs resolve a double-source energy budget (e.g. Sellers et al., 1987) and implement a multi-layer soil diffusion scheme (e.g. Braud et al, 1995b). They can also explicitly simulate photosynthesis (Olioso et al., 1996) and its functional coupling with plant transpiration and they represent vegetation dynamics (Calvet et al., 2008; Egea et al., 2011). Progress in LSMs led to more accurate estimations of energy and water fluxes. This resulted in more realistic simulations of air temperature and humidity of the surface boundary layer in atmospheric models (Noilhan et al., 2011). The improvement of the surface water budget in hydrological models permitted more accurate streamflow forescast (Habets et al., 2008) and drought monitoring (Vidal et al., 2010b). LSMs also proved their usefulness for agronomy application such as irrigation monitoring (Olioso et al., 2005).

This work focuses on the evaluation of the evapotranspiration (ET) simulated from a land surface model over a crop site for a long period of time. ET has been recognized as one of the most uncertain term in the surface water balance (Dolman and de Jeu, 2010; Mueller and Seneviratne, 2014). Uncertainties in simulated ET may propagate large errors in both LSM-atmosphere and LSM-hydrological coupled models. ET uncertainties can arise from (1) errors in the large-scale datasets used to force LSMs, (2) shortcomings in the model structure and (3) errors in the parameter values. Since LSMs were originally designed to be coupled with

atmospheric or hydrological models over large areas, their parametrization is generally parsimonious and their spatial integration is generally based on coarse resolution (~1-10km) maps of parameters. Surface parameters drive a large part of LSM uncertainties and explain most discrepancies between models (Chen et al., 1997; Gupta et al., 1999; Olioso et al., 2002; Boone et al., 2004). The representation of cropland and their temporal dynamics over long period of time need to be improved in LSMs (Lafont et al., 2011; Bonan and Santanello, 2013). Past evaluation studies focused on particular crop types for limited periods of time. They disregarded the succession of crop and inter-crop periods and its impact on the simulated water balance over a long period of time.

The uncertainties in soil hydraulic properties can be large due to significant spatiotemporal variability (Braud et al., 1995a), uncertainties in the estimation method (Baroni et al., 2010; Steenpass et al., 2011) and scale mismatch between the local measurements and the operational scale of the model (Mertens et al., 2005). Errors in soil hydraulic properties can have significant impact on LSM simulations of ET and soil water content (Jacquemin et al., 1990; Braud et al., 1995a; Cresswell and Paydar, 2000). Their impact on the model can be larger than the structural model uncertainties (Workmann and Skaggs, 1994; Baroni et al., 2010). Since the soil hydraulic properties are rarely known over large areas, they are generally derived from empirical pedotransfer functions (PTF) which relate the soil hydrodynamic properties to readily available variables such as soil texture and bulk density (Cosby et al.,1984; Vereecken et al., 1989; Schaap et al., 2000). These functions may not be accurate enough to describe the spatial variability of the soil hydrodynamic characteristics across soil types and their impact on LSM simulations need to be assessed locally (Espino et al., 1996; Baroni et al., 2010).

In this study, the ISBA-A-gs version (Calvet et al., 1998) of the ISBA LSM (Noilhan and Planton, 1989) is considered. ISBA-A-gs includes a coupled stomatal conductance-photosynthesis scheme. Local site studies demonstrated that ISBA (Noilhan and Mahfouf, 1996) and ISBA-A-gs (Gibelin et al., 2008) are able to correctly simulate the diurnal and seasonal time course of energy fluxes and soil water content, over contrasted soil and vegetation types. More variable performances were obtained by Olioso et al., (2002) over wheat fields with possible underestimation of ET.

This paper aims at evaluating the ISBA-A-gs simulations of ET over a 12-year Mediterranean crop succession. We focus on key drivers of simulated ET:

- the soil moisture at saturation (θ_s) which is involved in the simulation of soil evaporation,
- the soil moisture at field capacity (θ_{fc}), the soil moisture at wilting point (θ_{wp}) and the maximum rooting depth ($Z_{root\text{-}zone}$, referred as rooting depth hereafter). These parameters define the maximum water stock available for the crop which controls the plant transpiration. The wilting point and the rooting depth are two crop-dependent parameters which can lead to large variations in time of the root-zone water reservoir over the crop succession (Wetzel et al., 1987; Verhoef and Egea, (2014)).

In the rest of the text, the term "soil parameter" refer to θ_s , θ_{fc}, θ_{wp} and $Z_{root\text{-}zone}$. The simulations are assessed over the Avignon 'Remote Sensing and Fluxes' crop site where 14 arable crop cycles and 14 inter-crop periods were monitored through continuous measurements of soil water content and surface fluxes between April 2001 and December 2012. We represent the succession of crop cycles and inter-crop bare soil periods in the simulations. We address the following aspects:

- The impact of crop rotation on the dynamics of ET and root-zone soil moisture.
- The overall performances of the ISBA-A-gs simulations achieved with the standard soil and vegetation parameters over a 12-yr Mediterranean crop succession.
- The relative influence of each soil parameter on the simulation of ET and its soil/vegetation components, over a crop succession through a sensitivity analysis.
- The impact of the method used to retrieve the soil parameters on simulated ET. We test pedotransfer function, laboratory measurement and field monitoring methods. While constant values in time of the soil parameters are generally used in LSM, we assess whether the representation of the variations in time of the wilting point and the maximum rooting depth over the crop succession improves the simulation of ET.
- The propagation of uncertainties in the soil parameters on ET predictions. We quantified it through a Monte-Carlo analysis and we compared it with the uncertainties

triggered by the mesophyll conductance which is a key above-ground vegetation parameter involved in the stomatal conductance.

In discussion, we explain how the investigated soil parameters influence the simulation of ET over the crop succession, we discuss the sources of uncertainties related to each soil parameter retrieval method and we put into perspective the model performances by quantifying the uncertainties in measured ET.

2. Site and measurements

2.1 Site characteristics

The "Remote sensing and flux site" of INRA Avignon[1] (France; 43°55'00.4"N 4°52'41.0"E (WGS84 system) ; alt=32m a.s.l) is characterized by a Mediterranean climate with a mean annual temperature of 14°C and a mean annual precipitation of 687 mm. Rainfall mainly occurs in autumn (43% of yearly rainfall). It is a flat agricultural field oriented north-south in the prevailing wind direction (Fig. 1). The field size is 1.9 ha. In this work, we study a 12-year crop succession from April 2001 to December 2012 (Fig. 2 and Table 1). The crop succession consists in a succession of winter arable crops (wheat, peas) and summer arable crops (sorghum, maize, sunflower). Periods between two consecutive crop cycles lasted ~1-1.5 month in the case of a summer crop followed by a winter crop and ~9-10 months in the reverse case. During inter-crop periods, the soil is mostly bare. Limited wheat regrowths occurred over short periods of time. Irrigation is triggered only for summer crops (every two years) and concerns the May-July period.

2.2 Field measurements

Soil moisture, plant characteristics and micrometeorological observations were continuously monitored over the 12-year crop succession. A map of the field with the location of the instruments is given in Fig. 1

Soil measurements

Neutron probe was used to retrieve volumetric soil moisture over 3 (0–1.90 m) soil profiles with a vertical resolution of 10 cm. To implement the measurements, 3 neutron probe access tubes, spaced 40 m apart, were installed along a north-south transect located at the centre of

1 https://www4.paca.inra.fr/emmah_eng/Facilities/In-situ-facilities/Remote-Sensing-Fluxes

the field. A calibration was done for every access tube and soil layer by relating neutron count rates to soil moisture measured by gravimetric method. The average soil moistures at given depth over the soil profiles were then used. The measurements were performed on a weekly basis.

Surface ground heat flux (G) was derived from 4 heat flux plate measurements located at 5 cm depth. One plate was located along the crop row and the others were equally spaced apart in the inter-row. We accounted for heat storage estimated from temperature and soil moisture measured within the 5 cm layer.

Plant measurements

Plant characteristics (leaf area index (LAI), height, biomass) were monitored over all the crop cycles between April 2001 and December 2012. Canopy height was measured every 10 d using a standard meter tape. Leaf Area Index and plant biomass were measured at key crop phenological stages (5 to 6 measurements per crop cycle) using destructive methods and sampling scheme adapted to each crop. LAI was retrieved using a planimeter device and plant biomass was measured using a high precision scale device. Plant characteristics were measured at 4 locations of the field (Fig. 2) to sample the within field variability. Average values were recorded. Vegetation height was linearly interpolated on a daily basis. Daily interpolation of LAI was achieved using a functional relationship between LAI and the sum of degree-days (Duveiller et al., 2011).

Micrometeorological measurements

Half-hourly observations of air temperature and humidity, wind speed, atmospheric pressure, were continuously monitored at a height of 2 m above the ground or the canopy from a micro-meteorological station located at the centre of the field. Cumulative rainfall were measured from a standard meteorological station located at 150 m apart from the centre of the field. Net radiation (RN) was computed from shortwave and longwave upwelling and downwelling radiations measured from a net radiometer device located at the centre of the field.

Sensible (H) and latent (LE) heat fluxes were computed from an eddy-covariance system. The latter was composed of a 3D sonic anemometer set up in 2001 and of an open-path gas (H_2O, CO_2) analyzer set up in November 2003. The system was monitored following the state of the art guidelines for cropland sites (Rebmann et al., 2012; Moureaux et al., 2012). Fluxes were

computed on 30-min intervals using the EDIRE software[2]. The flux data processing included spike detection on raw data and standard eddy-covariance corrections (coordinate rotation, density fluctuations, frequency-loss). The ECPP[3] software (Beziat et al., 2009) was used to discard spurious flux (e.g. friction velocity and footprint controls) and to apply the Foken et al., (2004) quality control tests on the temporal stationarity and the development of turbulence conditions. In this work, only the best quality class of data (Mauder et al., 2013) was used. An additional threshold of 100 $W.m^{-2}$ on the energy balance non-closure was applied to eradicate very inconsistent fluxes. Direct eddy-covariance measurements of LE are used over the 20 November 2003-18 December 2012 period. They represent 60% of the period (71% if we consider only daytime). When no direct measurement of LE was available (2001-2003 period), LE was estimated as the residue of the energy balance (LE=RN-G-H). Valid direct and indirect LE measurements represent 65% of the 25 April 2001 -18 December 2012 period (77% of daytime). Cumulative ET in mm over given period of time was computed from LE half-hourly measurements.

2.3 Soil properties

Table 2 presents the values of the soil parameters averaged over the 0-1.2m soil layer, where most of the root-zone processes occur. The soil moisture at saturation (θ_s) was derived from soil bulk density measurements performed within the 0-1.2 m layer at different field locations and times over the 12-year period. We used the average value of θ_s to be representative of the soil structure at the field scale at which the simulations were conducted. The soil moisture at field capacity (θ_{fc}) and wilting point (θ_{wp}) were retrieved using laboratory or field methods:

(1) Laboratory method: It consisted in adjusting a Brooks and Corey (1964) retention curve model over soil matric potential (h) and soil water content measured in laboratory. These measurements were obtained from the Richard pressure plate apparatus at matric potentials of −1, −2, −3, −5, −10, −30, −50, −100, and −150 m (Bruckler et al., 2004). They were collected for 3 soil layers at depths of 0-0.4 m, 0.4-0.8 m and 0.8-1.2 m. A retention model was adjusted for each soil layer and was used to retrieve θ_{fc} and θ_{wp} for each soil layer. θ_{wp} was computed for h=-150 m. Most studies

2 Robert Clement, © 1999, University of Edinburgh, UK
http://www.geos.ed.ac.uk/abs/research/micromet/EdiRe
3 Eddy Covariance Post Processing, Pierre Béziat, CESBIO, Toulouse, France

agree on this definition (Boone et al., 1999; Olioso et al., 2002). For w_{fc} two definitions were used. We estimated θ_{fc} at h=-3.3m which corresponds to the agronomic definition (Olioso et al., 2002) and for an hydraulic conductivity of K= 0.1 mm d^{-1} which can be found in hydrological applications (Wetzel and Chang, 1987; Bonne et al, 1999). θ_{wp} and θ_{fc} estimates were averaged over the 0-1.2 m soil profile and their values are reported in Table 2.

(2) Field method: θ_{fc} and θ_{wp} were inferred from field measurements of soil moisture. The time evolution of the root-zone (0-1.2m) soil moisture was analyzed over each crop cycle. Under Mediterranean climate, the root-zone soil moisture generally starts from a upper-level which approximates θ_{fc}. It generally reaches a lower-level at the end of the growing season which often approaches θ_{wp}. The typical evolution of the root-zone soil moisture over the growing season is illustrated in Fig. 5b for wheat. To be consistent with the previous method, we integrated the soil moisture measurements over the 0-0.4 m, 0.4-0.8 m and 0.8-1.2 m soil layers. θ_{fc} and θ_{wp} were estimated for each soil layer as the maximum and the minimum, respectively, soil moisture over the growing season. θ_{fc} and θ_{wp} values were averaged over the 0-1.2m soil profile for each crop cycle (Table 3). θ_{wp} varies from one crop to another, but its mean value is close to the one derived from the retention curve. θ_{fc} shows lower temporal variability but its mean value significantly differs from the retention curve estimate.

The maximum rooting depth ($Z_{root\text{-}zone}$) was estimated from the analysis of the evolution in time of the vertical profiles of soil moisture field measurements over the growing season of each crop period. $Z_{root\text{-}zone}$ was approximated by the depth at which the soil moisture change in time vanished (Table 3). We assumed that at a given depth, the time variations in soil moisture due to the vertical diffusion and gravitational drainage were smaller than those generated by the plant water uptake (Olioso, et al 2002). This is a reasonable hypothesis for low hydraulic conductivity soil as the one under study. The $Z_{root\text{-}zone}$ =1.85 m obtained for wheat in 2006 can be related to the dryness of the crop period (256 mm of rain). The shallower $Z_{root\text{-}zone}$=1.0 m obtained for wheat in 2008 can be related to the wetness of the crop period (500 mm of rain).

3. The ISBA-A-gs model

3.1 Model description

The ISBA model (Noilhan and Planton, 1989; Noilhan and Mahfouf, 1996) is developed at the CNRM/Météo France within the SURFEX surface modeling platform (Masson et al, 2013). In this study, we used the version 6.1 of SURFEX. ISBA relies on a single surface energy budget of a soil-vegetation composite. The surface temperature is simulated using the Bhumralkar (1975) and Blackadar (1976) force restore scheme for heat transfers. An horizontal soil/snow/ice/vegetation surface partitioning is used to simulate the evapotranspiration. The soil water transfers are simulated using a force-restore scheme adapted from Deardoff, (1977) with three reservoirs: the superficial layer of thickness d_{surf}=0.01 m designed to regulate the soil evaporation, the root-zone which extends from the surface to the depth $Z_{root\text{-}zone}$ and the deep reservoir which extends from the base of the root-zone to the total soil depth. The force restore coefficients were parameterized as a function of the soil hydrodynamic properties which were derived from the Brooks and Corey, (1966) retention model. θ_{fc} and θ_{wp} are defined for K=0.1mm d^{-1} and for h=-150m, respectively. The soil parameters are derived from clay and sand fractions using the ISBA pedotransfer functions. The latter were built upon on the Clapp and Hornberger (1978) soil texture classification using statistical multiple regressions (Noilhan and Laccarère, 1995). The force-restore equations and coefficient formulas are given in Boone et al., 1999. Regarding the vegetation processes, we used the A-gs version of ISBA (Calvet et al., 1998; Calvet et al., 2008). A-gs is a coupled stomatal conductance-photosynthesis scheme. It uses a CO_2 responsive parameterization of photosynthesis based on the model of Goudriaan et al. (1985) and modified by Jacobs et al. (1996). It computes the stomatal conductance as a function of the net assimilation of CO_2. The CO_2 mesophyll conductance at a leaf temperature of 25° (gm) is the main tunable parameter of the A-gs scheme (Calvet et al., 1998; Calvet et al., 2012). It represents the response curve of the light-saturated net rate of CO_2 assimilation to the internal CO_2 concentration. The simulation of the plant response to water stress (Calvet et al., 2000; Calvet et al., 2012) is mainly driven by the maximum root-zone water stock available for the plant (MaxAWC) which is defined by:

$$MaxAWC=Z_{root\text{-}zone}(\theta_{fc}-\theta_{wp}) \quad (1)$$

The model is parametrized through 12 generic land surface patches using the ECOCLIMAP-II database which provides the ISBA surface parameters for ~273 distinct land cover types over Europe (Faroux et al., 2013).

3.2 Model implementation at the Avignon site

The simulations were conducted at the field scale. ISBA-A-gs was run at a 5 min time step and 30 min outputs of the state variables were analyzed. Continuous simulations were performed from 25 April 2001 up to 18 December 2012. The 12-year period was split into sub-simulations corresponding to crop and inter-crop periods (Fig. 2). The simulation was initialized once on 25 April 2001 using *in situ* soil temperature and soil moisture measurements for each soil layer. To ensure the continuity between 2 contiguous sub-simulations, each sub-simulation was initialized using the simulated soil moisture and soil temperature of the last time step of the previous sub-simulation. The C3 crop patch was used to represent wheat, pea and sunflower. The C4 crop patch was used for maize and sorghum. Inter-crop periods were represented by the bare soil patch. ISBA-A-gs was driven by local meteorological observations. It was forced by *in situ* LAI and vegetation height measurements averaged over 10 days. Crop irrigation was not simulated by the model and the actual amount of irrigation water was added to the local rainfall. The simulations were designed to be representative of the field scale. The in situ soil and vegetation parameters used in the simulations correspond to field average.

4 Methodology

This paper focuses on the evaluation of the ISBA-A-gs simulations of ET over the 12-year crop succession of the Avignon site. We focus on key soil parameters for the simulation of ET:

- the soil moisture at saturation (θ_s) which is involved in the simulation of soil evaporation,
- the field capacity (θ_{fc}), the wilting point (θ_{wp}) and the rooting depth ($Z_{root\text{-}zone}$) which control the plant transpiration through MaxAWC (Eq. (1)). Table 3 shows that θ_{wp} and $Z_{root\text{-}zone}$ are two crop-dependent parameters which can trigger large variations in time of MaxAWC over the crop succession. The variations in time of θ_{fc} are much lower than for for θ_{wp} and $Z_{root\text{-}zone}$. We thus investigate the impact of

using time-variable θ_{wp} and $Z_{root\text{-}zone}$ parameters over the crop succession and we assume constant in time field capacity value.

Distinct simulations are performed and compared (Table 4) to test the influence of these soil parameters on simulated ET.

4.1 Simulation cases

The simulation *PTF* corresponds to the standard implementation of the model. The above-ground vegetation parameters, the rooting depth (1.5m) and the deep reservoir size (0.5 m) are provided by the ECOCLIMAP-II database (Gibelin et al., 2006; Faroux et al., 2013). The soil hydraulic properties (θ_s, θ_{fc} , θ_{wp}) are derived from the local soil texture using the ISBA pedotransfer functions (Noilhan and Laccarère, 1995). No local calibration of the standard parameters is performed to test the portability of the parameters over a typical Mediterranean crop succession. The soil parameters are constant over the crop succession.

The simulations *LAB*, $FIELD_{cst}$ and $FIELD_{var}$ use in situ values of $Z_{root\text{-}zone}$, θ_s, θ_{fc} and θ_{wp} (Table 4). The rest of parameters are those used in *PTF*. The $Z_{root\text{-}zone}$ value used in *LAB* and $FIELD_{cst}$ is the average value of the rooting depths estimated from the soil moisture measurements over each crop cycle (Section 2.2). Its value (1.5 m) is equal to the ECOCLIMAP-II value used in *PTF*. *LAB*, $FIELD_{cst}$ and $FIELD_{var}$ use the same field-average estimate of θ_s derived from soil bulk density measurements. They mainly differ in the method used to retrieve θ_{fc} and θ_{wp} :

- *LAB* uses θ_{fc} and θ_{wp} retrieved from the retention curve model established from laboratory measurements (Table 2). θ_{wp} corresponds to the matric potential h=-150 m. θ_{fc} corresponds to the hydraulic conductivity K=0.1 mm d^{-1} to be consistent with the definition used by the ISBA pedotransfer method (PTF case).
- $FIELD_{cst}$ and $FIELD_{var}$ use θ_{fc} and θ_{wp} estimated from the monitoring of field soil moisture measurements over each crop cycle (Table 3). $FIELD_{cst}$ use constant in time values of θ_{wp} and $Z_{root\text{-}zone}$. It takes their temporal average values computed over the crop succession (Table 3). $FIELD_{var}$ accounts for the variations in time of θ_{wp} and $Z_{root\text{-}zone}$ over the crop succession (Table 3). Both $FIELD_{cst}$ and $FIELD_{var}$ use the average value of θ_{fc} over the crop succession.

4.2 Experiment analyses

We conduct the following analyses:

The first analysis consists in assessing the impact of the crop succession on the dynamics of simulated and measured ET and $\theta_{root\text{-}zone}$.

In the second analysis, we assess the overall performances of the standard simulation PTF over the 12-year crop succession.

The third analysis aims at quantifying the influence of each soil parameter (θ_s, θ_{fc}, θ_{wp}) on ET over the crop succession. We conduct a sensitivity analysis based on the *PTF* case. The parameters are tested one by one. We do not explore the interactions between parameters which are investigated in the following analysis. We explore similar variations in θ_s, θ_{fc}, θ_{wp} around their standard values used in *PTF* (+/- 0.015, +/-0.03). We also investigate the sensitivity of simulated ET to errors in these parameters by testing their in situ values used in the $FIELD_{cst}$ experiment. We do not consider variations in $Z_{root\text{-}zone}$. If the latter lead to similar variations in MaxAWC (Eq. (1)) than those triggered by θ_{wp}, its impact on ET will be similar than the impact of θ_{wp}. In this work a 0.25 m variation in $Z_{root\text{-}zone}$ leads to similar increase in MaxAWC and transpiration than a decrease of θ_{wp} by 0.015 m^3 m^{-3}.

In the fourth analysis, we investigate the impact of the method used to retrieve θ_s, θ_{fc} and θ_{wp}. We compare the *PTF*, *LAB* and $FIELD_{cst}$ simulation cases. By comparing $FIELD_{cst}$ and $FIELD_{var}$, we evaluate whether the representation of the variation in time of the wilting point and the rooting depth over the crop succession improves the simulation of ET. Finally, we select the estimation method that leads to the best representation of ET over the crop succession at the field scale.

The last analysis consists in quantifying the propagation of uncertainties in the soil parameters on ET predictions. To assess the relative importance of the impact of uncertainties in the soil parameters, we compare it with the impact of uncertainties in the mesophyll conductance which is a key above-ground vegetation parameter involved in the simulation of the stomatal conductance and the transpiration (Calvet et al., 2012).

To address these issues, we conducted two Monte-carlo analyses to generate two ensembles of 100 ET simulations for the $FIELD_{cst}$ simulation case.

- The Monte-Carlo scheme was first applied to the soil parameters tested in this work ($Z_{root\text{-}zone}$, θ_s, θ_{fc} and θ_{wp}). We chose to represent the uncertainties in the soil parameters

by the temporal and spatial variability at the field scale quantified in Table 2 and 3. Their distribution is assumed to be Gaussian (Table 8).

- The Monte-Carlo was then applied to the mesophyll conductance (g_m). We assumed a Gaussian probability distribution function for g_m (Table 8). The mean is the standard value given by Gibelin et al., (2006) and used in *FIELD*$_{cst}$ and the standard deviation is derived from literature meta-analysis (Calvet et al., 2000; Calvet et al., 2004).

4.3 Simulation performance metrics

The simulations were qualitatively evaluated comparing measured and simulated ET cumulated over the 25 April 2001 -18 December 2012 period. Cumulative ET were concomitantly analyzed with the root-zone soil moisture ($\theta_{root\text{-}zone}$) changes in time over selected crop cycles or inter-crop periods to identify the deficiencies in ET modeling. Cumulative values were computed over the time steps for which valid ET measurements were available. Daily daytime ET (ET_d) were computed when 90% of daytime measurements were valid for each day.

The simulation performance scores were quantified using the Root Mean Square Error (RMSE), the bias (BIAS), the standard deviation of the differences between simulations and measurements (SDD) and the correlation coefficient (r). These metrics were applied to half-hourly energy fluxes, $\theta_{root\text{-}zone}$ and ET_d. They were computed over the 20 November 2003-18 December 2012 period using only direct eddy-covariance measurements of LE.

5 Results

5.1 *Impact of the crop succession on the dynamics of evapotranspiration and soil water content*

Figure 3 illustrates the influence of the succession of crop periods and bare soil inter-crop periods on the temporal evolution of simulated and measured ET and root-zone soil moisture ($\theta_{root\text{-}zone}$).

The early stages of crop periods show high $\theta_{root\text{-}zone}$ which results from rainfall for winter crops and irrigation in May-June for summer crops. Crop growing periods are marked by abrupt increases in ET which is related to plant transpiration. This is concomitant with the depletion

of $\theta_{root\text{-}zone}$ which usually reaches its lower level at the end of the crop cycles. Daily ET reaches its highest values at maximum LAI (up to ~ 6 mm day-1).

Inter-crop periods which follow winter crop cycles are characterized by a dry period in July-August. The low soil water content directly results from the crop water uptake during the previous crop cycle. The soil moisture reaches its upper level in fall which comprises 43% of yearly rainfall. During inter-crop periods, the cumulative rate of ET is low. It is mostly influenced by soil evaporation. Daily ET generally keeps values lower than 1.5 mm d^{-1} . Larger values can be obtained after heavy rain events.

This experiment shows that simulated soil evaporation represents 64 % of cumulative ET over 12 years. It comprises more than 50 % and 95 % of daily ET for 80 % and 60 % of the days, respectively. While plant transpiration may generate significant daily ET during crop growing periods, it concerns only short-time periods compared to soil evaporation.

5.2 Evaluation of the standard simulation (PTF) over the 12-year crop succession

5.2.1 Evaluation of energy fluxes

Table 5 shows the overall performances of simulated energy fluxes. RN is properly simulated (r=0.99) with a low RMSE of 28 W m^{-2}. The latter probably falls within the range of the expected measurement errors. H and LE show substantial RMSE (56 W m^{-2} for H and 52 W.m^{-2} for LE). LE has a negative bias of -12 W m^{-2}. H shows larger positive bias of 18 W m^{-2}. G is markedly overestimated during daytime (daytime bias of 28 W m^{-2}).

5.2.2 *Evaluation of simulated evapotranspiration*

Figure 3 shows large underestimation in ET simulated using the ISBA standard vegetation and soil parameters. The deficit in cumulative ET computed over 65% of the 12-year period amounts to 1490 mm (24% of the measured cumulative ET). The overall bias in daily ET is -0.24 mm d^{-1}. This results in an overestimation of the root-zone soil water content which has an overall positive bias of 0.024 $m^3 m^{-3}$.

Table 6 provides the performance scores for crop and inter-crop periods. The bias and RMSE are lower for inter-crop periods due to lower flux magnitude. The correlations for daily ET are 0.8 and 0.6 for crop and inter-crop periods, respectively.

For crop cycles, ET and $\theta_{root\text{-}zone}$ are generally properly simulated during the early growing period. ET underestimation occurs during the water stress periods at the end of the crop cycles. The simulated ET shows an early decrease compared to the measured ET. The resulting $\theta_{root\text{-}zone}$ is overestimated at the end of most crop cycles.

For inter-crop periods, ET is mainly underestimated over wet bare soils. Over dry soils, the magnitude of soil evaporation is low and falls within the range of measurement errors. The overestimation of $\theta_{root\text{-}zone}$ at the end of most crop cycles can propagate through the subsequent inter-crop period as illustrated in 2004 and 2006 in Fig. 3. The induced bias in $\theta_{root\text{-}zone}$ persists during the dry period and is generally removed at the rainy period.

5.3 Impact of the soil parameters on ET simulations

5.3.1 Sensitivity analysis

Figure 4 shows the impacts of variations in θ_s, θ_{fc} and θ_{wp} on cumulative ET, cumulative soil evaporation and cumulative transpiration over the 12 year simulation period.

θ_{fc} has the greatest impact on total ET, followed by θ_{wp} and θ_s. ET increases with increasing values of θ_{fc} while it decreases with increasing values of θ_{wp} and θ_s. Soil evaporation increases with increasing values of θ_{fc} and decreasing values of θ_s. θ_{fc} has a larger impact on soil evaporation than θ_s. Transpiration increases with increasing value of θ_{fc} and decreasing values of θ_{wp}. The impact of θ_{fc} on soil evaporation is larger than on transpiration. The impact of using in situ field values of the soil parameters instead of the pedotransfer estimates is the largest for θ_s, followed by θ_{fc} and θ_{wp}.

5.3.2 Impact of the estimation method

We compare the *PTF*, *LAB* and $FIELD_{cst}$ simulations cases.

Figure 5 shows the underestimation of ET and the concomitant overestimation of $\theta_{root\text{-}zone}$ at the end of the crop cycle for *PTF* achieved with the pedotransfer estimate of θ_{wp}. The use of the lower *in situ* θ_{wp} in $FIELD_{cst}$ leads to higher cumulative ET and greater depletion in $\theta_{root\text{-}zone}$ which are both in better agreement with measurements. No effects are observed for irrigated crops (e.g. maize in Fig. 6).

Figure 7 shows the underestimation of soil evaporation over wet bare soil for *PTF* achieved with the pedotransfer estimate of θ_s. For $FIELD_{cst}$, which was achieved with a lower *in situ* θ_s,

the soil evaporation is increased and the decrease in $\theta_{root\text{-}zone}$ is steeper than for *PTF* (day 255 to 295 in Fig. 7). This in better agreement with the measurements. The improvement of the simulated soil evaporation is also illustrated at the start of the Maize crop cycle in Fig. 6.

The low θ_{fc} value estimated from the laboratory retention curve at K=0.1mm $day^{-1}$and used in *LAB* leads to the underestimation of simulated ET (Fig. 7a and Table 6). MaxAWC is underestimated (Table 4). The use of θ_{fc} estimated from the soil moisture measurements in $FIELD_{cst}$ leads to better agreement between simulated and measured soil evaporation (Fig. 7a and Table 6) .

5.3.3 Impact of time-variable rooting depth and wilting point

We compare $FIELD_{cst}$ based on constant in time values of $Z_{root\text{-}zone}$ and θ_{wp} with $FIELD_{var}$ which uses time-variable values of these parameters. $FIELD_{cst}$ and $FIELD_{var}$ show similar cumulative ET over 12 years and close simulation performances (Table 6). The use of $Z_{root\text{-}zone}$ estimated for each crop cycle can locally improve the simulation of ET. This is observed for the dry wheat cycle in 2006 (Fig. 5a) for which the actual rooting depth (1.85 m) is much greater than the 1.5 m mean value used in $FIELD_{cst}$. The use of θ_{wp} estimated for each crop cycle has little impact.

5.3.4 Selection of the best simulation over the crop succession

The *FIELD* cases achieved with the soil parameters derived from the field soil moisture measurements show substantial reductions in biases in LE, daily ET and $\theta_{root\text{-}zone}$ compared to PTF (Table 6). $FIELD_{cst}$ achieved with the average values of the soil parameters shows the lowest biases in ET. The deficit in cumulative ET over 12-yr which amounts to 24% for *PTF* is reduced to 6.7 % for $FIELD_{cst}$. It is 22% for *PTF* and 0.45% for $FIELD_{cst}$ if only direct measurements of LE are used over the 2004-2012 period. Figure 8 shows that $FIELD_{cst}$ properly reproduces the time evolution of measurements over the crop succession.

The RMSE for LE and daily ET are not reduced in $FIELD_{cst}$ compared to *PTF*. They mostly represent random differences between measurements and simulations. For $FIELD_{cst}$, the standard deviation of these random differences amounts to 53 W m^{-2}

5.4 Impact of uncertainties in situ soil parameters and comparison with the mesophyll conductance

We represent the uncertainties in simulated ET using cumulative values over the 2004-2012 period for which direct ET measurements are available. We display the simulation $FIELD_{cst}$, the ensemble of the Monte-Carlo simulations and the 95% percentile interval of simulated ET. The percentiles are computed over the empirical distribution of cumulative ET values. Fig 8 shows:

- The spatiotemporal variability of the soil parameters can generate large uncertainties in ET. The 95% percentile interval represents 867 mm (23%) of cumulative ET over 12 years.
- The uncertainties in the mesophyll conductance have a lower impact. The 95% percentile interval represents 70 mm (2%) of cumulative ET over 12 years.

6 Discussion

We tested 3 types of soil parameter estimates derived from:

- the ISBA pedotransfer functions,
- the retention curve model adjusted over laboratory measurements,
- the analysis of field measurements of soil moisture vertical profiles.

First, we explain the role of the investigated soil parameters in the simulation of soil evaporation and plant transpiration to understand how they influence the simulation of ET over the crop succession. Then, we discuss the sources of uncertainties related to each soil parameter retrieval method. Finally, we put into perspective the simulation performances obtained in this work by discussing the uncertainties in measured ET.

6.1 Impact of the soil parameters on simulated ET over the crop succession

Impact on soil evaporation

Soil evaporation decreases with increasing value of soil moisture at saturation (θ_s). This is related to the modelled superficial hydraulic diffusivity which decreases with increasing value

of θ_s (see Eq. (B4) in Appendix B). This depletes the superficial soil moisture and the resulting soil evaporation is reduced (Eq. (B4) in appendix B).

Soil evaporation increases with increasing field capacity (θ_{fc}) values. θ_{fc} increases the upper level of $\theta_{root\text{-}zone}$ during wet bare soil period, leading to increased capillary rise supply of the superficial soil moisture and enhanced soil evaporation (Eq. B5 in Appendix B).

Impact on transpiration

The field capacity and the wilting point, (θ_{wp}) have similar effects on plant transpiration through their symmetrical role in the water stock available for the crop's growth (MaxAWC, Eq. (1)). Transpiration increases with increasing value of MaxAWC. When MaxAWC is underestimated due to the overestimation of θ_{wp} (*PTF* simulation) or the underestimation of θ_{fc} (*LAB* simulation), early water stress is simulated which conducts to the underestimation of the simulated plant transpiration at the end of the crop cycle. This effect is not observed for irrigated crops (e.g. maize in Fig. 6) and rainy crop cycles. In these cases, the supply of water by irrigation is sufficient to satisfy crop water needs over the growing season. θ_{wp} is not reached and no water stress occurs.

Hierarchy of the impact of the soil parameters

The soil moisture at field capacity (θ_{fc}) is largely the most influencing soil parameter on the simulation of ET over the crop succession. This is due to its impact on both soil evaporation and transpiration. It is followed by the wilting point (θ_{wp}) and the soil moisture at saturation (θ_s) which have smaller effects.

The dynamics of crop rotation leads to long inter-crop periods between winter and summer crops. As a result, soil evaporation is the prevailing component of ET over the crop succession which explains the high sensitivity of ET to uncertainties in θ_{fc} and θ_s despite the low magnitude of soil evaporation flux.

6.2 Uncertainties in the soil parameters

6.2.1 Pedotransfer estimates

Most of ET underestimation reported for the standard implementation of the model (*PTF*) is due to the overestimation of both the soil moisture at wilting point and the soil moisture at saturation by the ISBA pedotransfer functions (Table 4). The error in θ_s is the largest and has the strongest impact on ET. The use of in situ values of θ_s and θ_{wp} in $FIELD_{cst}$ substantially reduces the bias in ET (Fig. 8). The deficit in simulated ET triggers an increase of the simulated drainage that is probably overestimated. The increase in simulated ET from *PTF* to $FIELD_{cst}$ is 1375 mm over 12 years. The decrease in simulated drainage is 1418 mm.

Large discrepancies have been reported between pedotransfer functions (PTFs) which are prone to distinct sources of uncertainties (Espino et al., 1996; Baroni et al., 2010; Gijsman et al., 2013). The first shortcoming concerns their representativeness of soil property variability. The ISBA pedotransfer functions were established upon the Clapp and Hornberger (1978) database. These functions were calibrated using mean values of soil properties over few classes of soil texture and do not represent the variability within each soil class. Besides maps of soil texture may not be accurate enough at regional scale. The second source of uncertainty is related to the estimation method. PTFs were designed to be applied over readily available variables such as soil texture. Improvements of the prediction equations may require the use of additional predictors related to soil structure (Vereecken et al, 1989). Most PTFs are based on simple statistical regressions such as the ISBA ones (Noilhan and Laccarère, 1995). The more advanced ROSETTA PTF (Schaap et al., 2001) addresses the uncertainty in the predicted soil parameters through the use of an ensemble of functions calibrated over distinct soil datasets. Such model provides essential information on the variance and covariance of the hydraulic properties (Scharnagl et al., 2011) which are required to propagate the uncertainties in the LSM simulations.

6.2.2 Laboratory estimates

The θ_{fc} estimate at K=0.1 mm d^{-1} used in *LAB* is too low and leads to the underestimation of of both soil evaporation and transpiration. This partly compensates for the increase in soil evaporation triggered by the use of in situ θ_s and explains that the resulting soil evaporation of LAB keeps values close to the PTF soil evaporation in Fig. 7a. The definition of θ_{fc} for K=0.1 mm d^{-1} is not appropriate to represent crop water needs.

Various studies have questioned the use of hydraulic properties inferred from laboratory techniques to simulate water transfers at the field scale (Basile et al., 2003; Mertens et al., 2005; Scharnagl et al., 2010). Laboratory experiments may not be representative of field conditions. Gravimetric measurements can disturb the actual soil structure. Small soil samples cannot capture the spatial and vertical heterogeneity of the soil structure at the field scale which can be substantially influenced by macroporosity and soil operations (Mertens et al., 2005). Single measurement cannot resolve the changes in soil structure caused by crop development and tillage operations (Baroni et al., 2010).

6.2.3 Field estimates

The most accurate simulation is achieved with the average values of $Z_{root\text{-}zone}$, θ_{fc} and θ_{wp} derived from the analysis of soil moisture measurements over each crop cycle ($FIELD_{cst}$). Field measurements of soil moisture better resolve the intra-field spatial variability through 4 neutron probes compared to the laboratory measurements. The analysis in time of the vertical profiles of soil moisture over the growing season provides meaningful estimates of the wilting point, the field capacity and the rooting depth for each crop cycle. Their mean values are accurate enough to represent the crop water needs and accurately simulate ET at the field scale over the 12-year crop succession. The variations in time of wilting point and rooting depth over the crop succession are low and their representation in the simulation has little impact on the overall model performances. The use of constant soil depths over the crop succession is preferable to ensure the conservation of mass in the force-restore simulation of the water balance over a long period of time. To account for time-variable rooting depth, an explicit soil multi-layer diffusion scheme would be required.

However, one can question the representativeness of field average in situ estimates of soil parameters which can be spatially and temporally variable. For example, the soil moisture at saturation is prone to large spatiotemporal variations due to macroporisity and impact of soil operations on the structure of the 0-0.4 m soil layer. We showed in Fig. 8 that the spatiotemporal variability in the soil parameters can generate large uncertainties in simulated ET over 12 years. These uncertainties are much larger than those generated by the mesophyll conductance. This is consistent with the findings of Calvet et al., (2012) who showed that ISBA-A-gs simulations are more sensitive to the root-zone reservoir (MaxAWC) than the

mesophyll conductance. However, our results depend on the assumptions made on the distributions of the tested parameters. The selected ranges of variations in the soil parameters are representative of the spatial variations in soil depth and soil structure according to our knowledge of the site. However, the spatial variability of these parameters should be properly quantified using adequate spatial sampling protocols and geostatistic methods (Garrigues et al., 2006). Besides, the variations in the soil hydrodynamic parameters may be larger when the model is integrated at regional scale (Braud et al., 1995). Finally, other vegetation parameters (e.g. water stress parameters, Verhoef and Egea., (2014)) may be source of uncertainties and should be investigated in further works.

6.3 Uncertainties in eddy covariance measurements

Random errors in eddy covariance measurements arise from turbulence sampling errors, instrument errors and flux footprint uncertainties (Richardson et al., 2006). We applied the Richardson et al. (2006) method (explained in Appendix C) to compute the standard deviation of the measurement random error for various classes of LE values. Results are given in Table B1. Random errors are very likely to cancel out when measurements are cumulated over long period of time. However, they can explain a large part of the unresolved random differences between the simulations and the measurements at half-hourly and daily time scales.

Eddy-covariance are also prone to systematic errors. Particularly, the eddy-covariance system could fail to resolve low frequency turbulence structures that could lead to the underestimation of eddy fluxes (Foken, 2008). This results in the non closure of the measured energy balance (EB) which is a critical source of uncertainties when these measurements are compared to LSM simulations. Other reasons for the EB non-closure include horizontal and vertical advection, inaccuracies in the eddy covariance processing and footprint mismatch between the eddy fluxes and the other energy fluxes (RN,G) (Foken, 2008; Leuning et al., 2012). The application of an energy imbalance threshold of 100 $W.m^{-2}$ minimized the magnitude of the EB non-closure of our dataset. The mean and the standard deviation of the absolute value of the EB non-closure are 28 $W.m^{-2}$ and 22 $W.m^{-2}$, respectively. This is comparable to the non-closure reported for cropland in Wilson, et al. (2002); Hendricks et al. (2010) and Ingwersen et al. (2010).

The uncertainties in eddy-covariance measurements are further assessed comparing the direct measurement of LE with two other estimates. The first estimate is computed as the residue of the energy balance assuming that H is error-free. The second estimate is derived from the bowen ratio (ratio between H and LE) assuming that the bowen ratio is correctly estimated (Twine et al., 2000). The SD of the differences in LE between the direct measurement and the other estimates fall between 24 and 36 W m^{-2} (Table 7). The MD at half-hourly time scale fall between 3 and 7 W m^{-2}. The MD in cumulative ET over 12 years between the bowen ratio estimate and the direct measurement represents 727 mm (12%). It is 310 mm (5%) between the estimate derived from the residue of the energy balance and the direct measurement. The deficits in simulated ET reported in this work are thus probably larger due to likely underestimation of ET by eddy-covariance measurements.

7 Summary

In this study, the SURFEX/ISBA-A-gs simulations of evapotranspiration (ET) are assessed at the field scale over a 12-year Mediterranean crop succession. The model is evaluated in its standard implementation which relies on the use of the ISBA pedotransfer function estimates of the soil properties. The analysis focuses on key parameters which drive the simulation of ET, namely the rooting depth, the soil moisture at saturation, the soil moisture at field capacity and the soil moisture at wilting point. A sensitivity analysis is first conducted to quantify the relative contribution of each parameter on ET simulated over the crop succession. The impact of the estimation method used to retrieve the soil parameters (pedotransfer function, laboratory and field methods) on ET is then analyzed. The benefit of representing the variations in time of the rooting depth and the wilting point is evaluated. Finally, the propagation of uncertainties in the soil parameters on ET simulations is quantified through a Monte-Carlo analysis and compared with the uncertainties triggered by the mesophyll conductance which is a key above-ground driver of the stomatal conductance.

Evapotranspiration mainly results from the soil evaporation when it is simulated over a succession of crop cycles and inter-crop periods for Mediterranean croplands. The crop transpiration generates high ET over short-time periods while the soil evaporation represents more than 50% of ET for 80% of the days. This results in a high sensitivity of simulated evapotranspiration to uncertainties in the soil moisture at field capacity and the soil moisture at saturation which both drive the simulation of soil evaporation. Field capacity was proved

to be the most influencing parameter on the simulation of evapotranspiration over the crop succession due to its impact on both transpiration and soil evaporation.

ET simulated with the standard surface and soil parameters of the model is largely underestimated. The deficit in cumulative ET amounts to 24% over 12 years. The bias in daily daytime ET and root-zone soil moisture are -0.24 mm $d^{-1}$and 0.024 m^3 m^{-3}. ET underestimation is mainly related to the overestimation of the soil moisture at saturation and the soil moisture at wilting point by the ISBA pedotransfer functions. The overestimation of the wilting point triggers the underestimation of the water stock available for the crop's growth which conducts to the underestimation of the simulated plant transpiration at the end of the crop cycle. The overestimation of the soil moisture at saturation triggers an underestimation of the water diffusivity in the superficial layer which reduces the soil evaporation during wet periods.

The field capacity estimate derived from laboratory measurements at K=0.1 mm day^{-1} is too low and leads to the underestimation of evapotranspiration. This is related to the lack of representativeness of the soil structure variability by the laboratory samples and inappropriate definition of the field capacity at K=0.1 mm day^{-1} to represent crop water needs.

The most accurate simulation is achieved with the average values of the soil parameters derived from the temporal analysis of field measurements of soil moisture vertical profiles over each crop cycle. The representation of the variations in time of the wilting point and the maximum rooting depth over the crop succession has little impact on the ET simulation performances.

The uncertainties in the soil parameters, related to the use of field average estimates, generate substantial uncertainties in simulated ET (the 95% confidence interval represents 23% of cumulative ET over 12-years) which are much larger than the uncertainties triggered by the mesophyll conductance.

The measurement random errors tend to cancel out when measurements are cumulated over long period of time. They explain a large part of the unresolved scattering between simulations and measurements at half-hourly time scale. The deficits in simulated ET reported

in this work are probably larger due to likely underestimation of ET by eddy-covariance measurements.

Other model shortcoming could concern the lack of root profile representation in the force-restore water transfer scheme which can affect the representation of the effect of water stress on plant transpiration (Desborough et al., 1997; Braud et al., 2005; Fan et al., 2006). A multi-layer diffusion scheme may represent the soil vertical heterogeneity and the interactions between plant and soil more accurately. However, the performances of such detailed models rely on accurate parametrization of root profile and soil vertical heterogeneity which may trigger larger uncertainties in ET. Other sources of uncertainties in the model structure include inaccurate ET partitioning between the soil and the vegetation at low LAI which may require a double-source energy balance (Olioso et al., 2002), inaccurate representation of the resistance of a drying soil to water vapor diffusion which depends on both soil structure and texture (Kondo et al., 1990; Merlin et al, 2011) and shortcomings in the parametrization water stress functions (Verhoef et al., 2014).

Finally, this work highlights the prevailing role of the soil parameters in the simulation of ET dynamics over a multi-year crop succession. Accounting for uncertainties in soil properties is of paramount importance for the spatial integration of land surface models. Methods need to be developed to spatially retrieve the soil parameters and their uncertainties at regional scale. We showed that pedotransfer functions can be inaccurate. Field measurements of soil moisture are generally not available at regional scale. Satellite observations of soil moisture and vegetation status offer great promise to retrieve the soil properties over large areas. Bayesian inverse modelling are appropriate approaches to calibrate the soil parameters and translate their uncertainties into uncertainties in the simulated fluxes (Mertens et al., 2004; Vrugt et al., 2009; Scharnagl et al., 2011). All sources of modelling (forcing data, vegetation and soil parameters, model structure) and measurement uncertainties can be adequately incorporated in the analysis. Our results will serve as a basis to implement such method in order to monitor ET and its uncertainties over cropland.

APPENDICES

Appendix A Definition of the main symbols

BIAS: Mean difference between simulated and measured values

E: Soil evaporation (mm)

EB: Energy balance

ET: Cumulative evapotranspiration (mm)

ET_d: Daily daytime evapotranspiration (mm d^{-1})

FIELD: Simulation case achieved with θ_{fc} and θ_{wp} retrieved from the temporal analysis of field soil moisture measurements

G: Ground heat flux (W m^{-2})

h: Matric potential (m)

H: Sensible heat flux (W m^{-2})

K: Hydraulic conductivity (m s^{-1})

$K_{s:}$ Hydraulic conductivity at saturation (m s^{-1})

LAB: Simulation case achieved with θ_{fc} and θ_{wp} retrieved from laboratory methods

LE: Latent heat flux (W m^{-2})

MaxAWC: Maximum root-zone water stock available for the crop (mm)

MD: Mean difference

Meas: Measurement

PTF: Pedotransfer function

PTF: Simulation case achieved with θ_s, θ_{fc}, θ_{wp} , retrieved from the ISBA pedotransfer function

RMSE: root mean square error between simulated and measured values

RMSD: root mean square difference between two simulations or two types of measurement

RN: Net radiation (W m^{-2})

SDD: standard deviation of the differences between two simulations or two types measurement

T: transpiration flux (mm)

$Z_{root\text{-}zone}$: Rooting depth (m)

θ_{fc} : volumetric soil moisture at field capacity ($m^3\,m^{-3}$)

$\theta_{root\text{-}zone}$: root-zone volumetric soil moisture (0-d_2) ($m^3\,m^{-3}$)

θ_{sat} : volumetric soil moisture at saturation ($m^3\,m^{-3}$)

θ_{surf} : superficial volumetric soil moisture (0-0.01m) ($m^3\,m^{-3}$)

θ_{wp} : volumetric soil moisture at wilting point ($m^3\,m^{-3}$)

Appendix B : The soil evaporation in the force-restore scheme

The ISBA soil evaporation (E) is given by

$$E=(1-veg)\rho_a C_H V[h_u q_{sat}-q_a] \quad \text{(B1)}$$

where veg is the fraction of vegetation cover, ρ_a is the dry air density, C_H is the drag coefficient, V is the wind speed, q_{sat} is the surface specific humidity at saturation and q_a is the air specific humidity at the reference height. h_u is the air relative humidity at the surface and is computed as :

$$h_u=0.5[1-\cos(min(\frac{\theta_{surf}}{\theta_{fc}},1)\pi)] \quad \text{(B2)}$$

where θ_{surf} is the superficial soil moisture and θ_{fc} is the soil moisture at field capacity. E is at its potential rate when $\theta_{surf}>\theta_{fc}$ (hu=1). It depletes as θ_{surf} drops below θ_{fc}. For h_u $q_{sat}<q_a$, if $q_{sat}< q_a$ a dew flux is triggered and if $q_{sat}> q_a$ the soil evaporation is set to zero.

The time course of θ_{surf} is given by the force-restore equation:

$$\frac{\partial\theta_{surf}}{\partial t}=\frac{C_1}{\rho_w d_1}(P-E)-\frac{C_2}{\tau}(\theta_{surf}-\theta_{eq}) \quad \text{(B3)}$$

In Eq. (B3), ρ_w is the liquid water density, P is the flux of water reaching the surface and τ is the restore constant of one day.

The coefficient C_1 is driving the moisture exchange between the surface and the atmosphere. It is an inverse function of the hydraulic diffusivity (Noilhan and Planton, 1989; Eq. B.4).

$$C_1=C_{1,s}d_{surf}(\frac{\theta_s}{\theta_{surf}})^{0.5b+1} \quad \text{(B4)}$$

In Eq. (B4), $C_{1,s}$ is the value at saturation (in m^{-1}) calibrated as a function of clay fraction and b is the slope of the Brooks and Corey, (1964) retention curve. C_1 is minimum at saturation and increases as the soil surface dries out. It reaches its maximum for $\theta_{surf}=\theta_{wp}$. For θ_{surf} lower than θ_{wp} , water vapor phase transfers are prevailing. C_1 is represented by a Gaussian formulation (Giordani et al., 1993; Giard and Bazile, 1996) and decreases with increasing soil temperature and decreasing soil moisture**.**

The second term in the right-hand side of Eq. (B3) represents the vertical water diffusion between the root-zone and the superficial layer. It is ruled by the diffusion coefficient C_2 (Eq. (B5)) which quantifies the rate at which the soil moisture profile between layer 1 and 2 is restored to the equilibrium θ_{eq} (water content at the balance between the gravity and the capillary forces).

$$C_2 = C_{2ref}\left(\frac{\theta_{root-zone}}{\theta_s - \theta_{root-zone} + \theta_l}\right) \qquad \text{(B5)}$$

In Eq. A5, $\theta_{root\text{-}zone}$ is the root-zone soil moisture, θ_1 is a numerical constant . C_{2ref} is the mean value of C_2 for $\theta_2=0.5\ \theta_s$ and is computed as a function of clay fraction. C_2 is an increasing function of $\theta_{root\text{-}zone}$.

In ISBA, the force-restore water transfer scheme and the resulting soil evaporation strongly depend on soil texture (Jacquemin et al, 1990). Coarse soil texture are characterized by high soil hydraulic diffusivity and conductivity which are represented in the model by low C_1 and high C_2, respectively. For sandy soil, low value of C_1 reduces the depletion of θ_{surf} due to soil evaporation and high C_2 enhances the supply of θ_{surf} by capillary rises. The resulting daily variations of θ_{surf} are low and the values of θ_{surf} are frequently higher than θ_{fc}. The resulting soil evaporation is frequently at its potential rate. Conversely, clay soils have higher C_1 and lower C_2. This leads to more rapid depletion of θ_{surf} which keeps lower values compared to sandy soil. The subsequent soil evaporation drops since it is more rapidly limited by the soil water supply.

Appendix C: Characterization of the random errors in the eddy covariance measurements

The Richardson et al. (2006) method to assess the random errors in eddy-covariance measurements consists in selecting 24h apart pairs of measurements acquired under equivalent environmental conditions. The latter are defined by differences in vapor pressure deficit within 0.15kPa, wind speed within 1m.s^{-1}, air temperature within 3°C and photosynthetic photon flux within 75 µmol.m^{-2}.s^{-1}. Compared to the original method, additional criteria were implemented: wind direction within +/-15°, footprint within 30%, surface soil moisture within 0.03 m^3.m^{-3}, incoming solar radiation within 50 W.m^{-2}. The measurement pairs (x_1 and x_2) are assumed to be two measurements of the same flux F at two distinct times.

$$x_1 = F + \delta_1 \quad \text{(B1)}$$

$$x_2 = F + \delta_2 \quad \text{(B2)}$$

δ represents the random error which is assumed to be uncorrelated in time and identically distributed in time. Richardson et al. (2006) showed that the standard deviation of the random error (σ_δ) is :

$$\sigma_\delta = \sigma(x_1 - x_2)/\sqrt{2} \quad \text{(B3)}$$

where $\sigma(x_1\text{-}x_2)$ is the standard deviation of the differences between the values of the measurement pairs. In our experiment, we assume that x_1 -x_2 follows a Gaussian distribution. Table C.1 provides σ_δ computed for distinct classes of LE values.

Table C1: Standard deviation (σ_δ) of the random error of the LE measurements computed for distinct classes of LE values. N is the number of measurement pairs used to estimate the random error.

	Ranges of LE flux ($W.m^{-2}$)					
	< 0	[0,50]	[50,100]	[100,200]	>200	
N	627	2592	615	233	117	
σ_δ	4.8	7.8	14.9	23.4	53.4	

References

Arora, V.K.: Modeling vegetation as a dynamic component in soil- vegetation-atmosphere transfer schemes and hydrological models, Rev. Geophys., 40(2), 1006, 2002.

Basile, A., Ciollaro, G., and Coppola, A.: Hysteresis in soil water characteristics as a key to interpreting comparisons of laboratory and field measured hydraulic properties, Water Resour. Res., 39, 1355, doi:10.1029/2003WR002432, 2003.

Baroni, G., Facchi, a., Gandolfi, C., Ortuani, B., Horeschi, D., van Dam, J.C.: Uncertainty in the determination of soil hydraulic parameters and its influence on the performance of two hydrological models of different complexity, Hydrol. Earth Syst. Sci. 14, 251–270, 2010.

Beziat, P., Ceschia, E., Dedieu, G.: Carbon balance of a three crop succession over two cropland sites in South West France, Agr. Forest Meteorol., 149, 1628-1645, 2009.

Bhumralkar, C. M.: Numerical experiments on the computation of ground surface temperature in an atmospheric general circulation model, J. Appl. Meteorol., 14, 1246–1258, 1975

Blackadar, A. K.: Modeling the nocturnal boundary layer. Preprints, Third Symp. on Atmospheric Turbulence, Diffusion and Air Quality, Raleigh, NC, Amer. Meteor. Soc., 46–49, 1976.

Bonan,G.: Land surface processes in climate models. In Ecological Climatology, Ed Bonan, G. Cambridge, 2010.

Bonan, G B., Santanello, J.A.: Modelling the land-atmosphere interface across scales: from atmospheric science to Earth system science, ILEAPS newsletter, 13, 6-8, 2013.

Boone, A., Calvet, J.-C., Noilhan, J.: Inclusion of a Third Soil Layer in a Land Surface Scheme Using the Force–Restore Method, J. Appl. Meteorol., 1611-1630, 1999.

Boone, A. and coauthors: The Rhone-Aggregation Land Surface Scheme Intercomparison Project: An Overview, J. Climate, 187-208, 2004.

Braud I., Dantas-Antonio, A.C., Vauclin,M. : A stochastic approach to studying the influence of the spatial variability of soil hydraulic properties on surface fluxes, temperature and humidity. J. Hydrol., 165, 283-310, 1995a.

Braud, I., Dantas-Antonino, A.C., Vauclin, M., Thony, J-L., Ruelle, P.: A simple soil-plant atmosphere transfer model (SiSPAT) development and field verification, J. Hydrol., 166, 213-250, 1995b.

Braud, I., Varado, N., Olioso, A. : Comparison of root water uptake modules using either the surface energy balance or potential transpiration, J. Hydrol., 301, 267–286, 2005.

Brooks, R. H., and Corey, A.T.: Properties of porous media affecting fluid flow, J. Irrig. Drain. Amer. Soc. Civil Eng., 2, 61–88, 1966.

Bruckler, L., Lafolie, F., Doussan, C., Bussières, F.: Modeling soil-root water transport with non-uniform water supply and heterogeneous root distribution, Plant and Soil, 260, 205-224, 2004.

Calvet, J.-C., Noilhan, J., Roujean, J-L., Bessemoulin, P., Cabelguenne, M., Olioso, A., Wigneron, J-P.: An interactive vegetation SVAT model tested against data from six contrasting sites, Agr. Forest Meteorol., 92, 73-95, 1998.

Calvet, J.-C.: Investigating soil and atmospheric plant water stress using physiological and micrometeorological data. Agr. Forest Meteorol., 103, 229-247, 2000.

Calvet, J.-C., V. Rivalland, C. Picon-Cochard, and Guehl, J.-M. : Modelling forest transpiration and CO 2 fluxes - Response to soil moisture stress, Agric. For. Meteorol., 124, 143 – 156, 2004

Calvet, J.-C., Gibelin, A.-L., Roujean, J.-L., Martin, E., Moigne, P. L., Douville, H., Noilhan, J.: Past and future scenarios of the effect of carbon dioxide on plant growth and transpiration for three vegetation types of southwestern France, Atmospheric Chemistry and Physics, 8, 397-406, 2008.

Calvet, J.-C., Lafont, S., Cloppet, E., Souverain, F., Badeau, V., Le Bas, C.: Use of agricultural statistics to verify the interannual variability in land surface models: a case study over France with ISBA-A-gs, Geoscientific Model Development, 5, 37-54, 2012.

Chen, T. H., and Coauthors: Cabauw experimental results from the project for intercomparison of land-surface parameterization schemes, J. Climate, 10, 1194–1215, 1997.

Clapp, R., Hornberger, G.: Empirical equations for some soil hydraulic properties. Water Resour. Res., 14, 601–604, 1978.

Cosby, B. J., G. M. Hornberger, R. B. Clapp, Ginn, T.R.: A statistical exploration of the relationships of soil moisture characteristics to the physical properties of soils, Water Resour. Res., 20, 682–690, 1984.

Cresswell, H. P. and Paydar, Z.: Functional evaluation of methods for predicting the soil water characteristic, J. Hydrol., 227, 160– 172, 2000.

Deardorff, J. W.: A parameterization of ground surface moisture content for use in atmospheric prediction models, J. Appl. Meteorol., 16, 1182–1185, 1977.

Decharme, B., Douville, H., Boone, A.; Habets, F., Noilhan, J.: Impact of an Exponential Profile of Saturated Hydraulic Conductivity within the ISBA LSM: Simulations over the Rhône Basin, J. Hydrometeorol., 61-80, 2006.

Decharme, B., Boone, a., Delire, C., Noilhan, J.: Local evaluation of the Interaction between Soil Biosphere Atmosphere soil multilayer diffusion scheme using four pedotransfer functions, J. Geophys. Res., 116, D20126, 2011.

Demarty, J., Ottlé, C., Braud, I., Olioso, A., Frangi, J-P., Bastidas, L.A., Gupta, H.: Using a multiobjective approach to retrieve information on surface properties used in a SVAT model, J. Hydrol., 287, 214-236, 2004.

Desborough, C.E., Pitman, A., Irannejad, P.: Analysis of the relationship between bare soil evaporation and soil moisture simulated by 13 land surface schemes for a simple non-vegetated site, Global and Planetary Change 13, 47–56, 1996.

Desborough, C.E.: The Impact of Root Weighting on the Response of Transpiration to Moisture Stress in Land Surface Schemes, Monthly Weather review, 1920–1930, 1997.

Dolman, A.J, De Jeu, R. A. M. : Evaporation in Focus. Nature Geosciences, 3, 296, 2010.

Duveiller, G., Weiss, M., Baret, F., Defourny, P.: Retrieving wheat Green Area Index during the growing season from optical time series measurements based on neural network radiative transfer inversion, Remote Sens. Environ., 115, 887-896, 2011.

Egea, G., Verhoef, A., Vidale, P. L.: Towards an improved and more flexible representation of water stress in coupled photosynthesis-stomatal conductance models. Agr. Forest Meteorol., 151, 1370-1384, 2011.

Espino, A., Mallants, D., Vanclooster, M., Feyen, J.: Cautionarynotes on the use of pedotransfer functions for estimating soil hydraulic properties, Agric. Water Manage., 29, 235– 253, 1996.

Fan, Y., Van den Dool, H. M., Lohmann, D., Mitchell, K.: 1948–98 U.S. hydrological reanalysis by the NOAH land data assimilation system, J. Climate, 19, 1214–1237, 2006.

Faroux, S., Kaptué Tchuenté, A. T., Roujean, J.-L., Masson, V., Martin, E., Le Moigne, P.: ECOCLIMAP-II/Europe: a twofold database of ecosystems and surface parameters at 1 km resolution based on satellite information for use in land surface, meteorological and climate models, Geosci. Model Dev., 6, 563-582, 2013.

Foken, T., Mauder, M., Mahrt, L., Amiro, B., Munger, W.: Post-field data quality control, in: Lee, X., et al. (Eds.), Handbook of Micrometeorology, 181–208, 2004.

Foken, T.: The energy balance closure problem: an overview, Ecological Applications, 18, 1351-1367, 2008.

Garrigues, S., Allard, D., Baret, F., Weiss, M.. Influence of landscape spatial heterogeneity on the non linear estimation of leaf area index from moderate spatial resolution remote sensing data. *Remote Sensing of Environment, 105* (4), 286-298. DOI : 10.1016/j.rse.2006.07.013, 2006.

Giard, D., Bazile, E.: Implementation of a New Assimilation Scheme for Soil and Surface Variables in a Global NWP Model, Monthly Weather Review, 997-1015, 2000.

Gibelin, A.-L., Calvet, J-C., Roujean, J-L., Jarlan, L., Los, S. O.: Ability of the land surface model ISBA-A-gs to simulate leaf area index at the global scale: Comparison with satellites products, J. Geophys. Res., 111, 1-16, 2006.

Gibelin, A.-L., Calvet, J.-C., Viovy, N.: Modelling energy and CO 2 fluxes with an interactive vegetation land surface model-Evaluation at high and middle latitudes, Agr. Forest Meteorol., 148, 1611-1628, 2008.

Giordani, H., Noilhan, J., Lacarrère, P., Bessemoulin, P., Mascart, P.: Modelling the surface processes and the atmospheric boundary layer for semi-arid conditions, Agr. Forest Meteorol., 80, 263-287, 1996.

Gijsman, A. J., Jagtap, S. S., and Jones, J. W.: Wading through a swamp of complete confusion: how to choose a method for estimating soil water retention parameters for crop models, Europ. J. Agronomy, 18, 77–106, 2003.

Goudriaan, J., van Laar, H. H., van Keulen, H., and Louwerse, W.: Photosynthesis, CO 2 and plant production, in: Wheat Growth and Modelling, edited by: Day, W. and Atkin, R. K., NATO ASI Series, Plenum Press, New York, Series A, 86, 107–122, 1985.

Gupta, H. V., Bastidas, L. a., Sorooshian, S., Shuttleworth, W.J., Yang, Z.L.: Parameter estimation of a land surface scheme using multicriteria methods, J. Geophys. Res., 104, 19491, 1999.

Habets, F., Boone, A., Champeaux, J. L., Etchevers, P., Franchisteguy, L., Leblois, E., Ledoux, E., Moigne, P. L., Martin, E., Morel, S., Noilhan, J., and Viennot, P.: The SAFRAN-ISBA-MODCOU hydrometeorological model applied over France, 113, 1-18, 2008.

Hendricks Franssen, H.J., Stöckli, R., Lehner, I., Rotenberg, E., Seneviratne, S.I.: Energy balance closure of eddy-covariance data: A multisite analysis for European FLUXNET stations, Agr. Forest Meteorol., 150, 1553-1567, 2010.

Ingwersen, J., Steffens, K., Högy, P., Zhunusbayeva, D., Poltoradnev, M., Gäbler, R., Wizemann, H., Fangmeier, A., Wulfmeyer, V.; Streck, T.: Comparison of Noah simulations with eddy covariance and soil water measurements at a winter wheat stand, Agr. Forest Meteorol., 151, 345-355, 2011.

Jacquemin, B., and Noilhan, J.: Sensitivity study and validation of a land surface parameterization using the hapex-mobilhy data set, Boundary Layer Meteorology, 52, 93-134, 1990.

Jarvis, P.G.: The interpretation of the variations in water potential and stomatal conductance found in canopies in the field, Philosophical Transactions of the Royal Society, London, Ser. B., 273, 593–610, 1976.

Jacobs, C. M. J., Van den Hurk, B. J. J. M., and De Bruin, H. A. R.: Stomatal behaviour and photosynthetic rate of unstressed grapevines in semi-arid conditions, Agr. Forest Meteorol., 80, 111–134, 1996

Kondo, J., Nobuko, S., Takeshi, S.: A parameterization of evaporation from bare soil surfaces, J. Appl. Meteor., 29, 385–389, 1990.

Lafont, S., Zhao, Y., Calvet, J., Peylin, P., Ciais, P., Maignan, F. and Weiss, M.: Modelling LAI, surface water and carbon fluxes at high-resolution over France: comparison of ISBA-A-gs and ORCHIDEE, Biogeosciences, 9, 439–456, 2012.

Leuning, R., Van Gorsel,E., Massman, W.J., Isaac, P.R.: Reflections on the surface energy imbalance problem, Agr. Forest Meteorol., 156, 65-74, 2012.

Mahfouf, J. F. and Noilhan, J.: Comparative Study of Various Formulations of Evaporations from Bare Soil Using In Situ Data. J. Appl. Meteor., 30, 1354–1365, 1991.

Masson, V, Champeaux, J-L., Chauvin, F., Meriguet, C., Lacaze, R: A global database of land surface parameters at 1-km resolution in meteorological and climate models, J. Climate, 16, 1261–1282, 2003.

Masson, V., Le Moigne, P., Martin, E., Faroux, S., Alias, A., Alkama, R., Belamari, S., Barbu, A., Boone, A., Bouyssel, F., Brousseau, P., Brun, E., Calvet, J.-C., Carrer, D., Decharme, B., Delire, C., Donier, S., Essaouini, K., Gibelin, A.-L., Giordani, H., Habets, F., Jidane, M., Kerdraon, G., Kourzeneva, E., Lafaysse, M., Lafont, S., Lebeaupin Brossier, C., Lemonsu, A., Mahfouf, J.-F., Marguinaud, P., Mokhtari, M., Morin, S., Pigeon, G., Salgado, R., Seity, Y., Taillefer, F., Tanguy, G., Tulet, P., Vincendon, B., Vionnet, V., and Voldoire, A.: The SURFEXv7.2 land and ocean surface platform for coupled or offline simulation of earth surface variables and fluxes, Geosci. Model Dev., 6, 929-960, 2013.

Mauder, M., Cuntz, M., Drüe, C., Graf, A., Rebmann, C., Schmid, H.P., Schmidt, M., Steinbrecher, R.: A strategy for quality and uncertainty assessment of long-term eddy-covariance measurements, Agr. Forest Meteorol. 169, 122–135, 2013.

Merlin, O., Al Bitar, A., Rivalland, V., Béziat, P., Ceschia, E., Dedieu, G.: An Analytical Model of Evaporation Efficiency for Unsaturated Soil Surfaces with an Arbitrary Thickness, Journal of Applied Meteorology and Climatology, 50, 457–471, 2011.

Mertens J, Madsen H, Feyen L, Jacques D, Feyen J.: Including prior information and its relevance in the estimation of effective soil parameters in unsaturated zone modelling. Journal of Hydrology, 294, 251 – 269, 2004.

Mertens, J., Madsen, H., Kristensen, M., Jacques, D., Feyen, J.: Sensitivity of soil parameters in unsaturated zone modelling and the relation between effective, laboratory and in situ estimates, Hydrol. Process., 19, 1611–1633, 2005.

Montaldo, N., and Albertson, J D.: On the Use of the Force–Restore SVAT Model Formulation for Stratified Soils, J. Hydrometeorology, 2, 571-578, 2001.

Moureaux C., Ceschia, E., Arriga, N., Beziat, P., Eugster., Kutsch, W L., Pattey, E.: Eddy covariance measurements over crops, in Aubinet, M., Vesala, T., Papale, D., (Eds), Eddy Covariance: A practical guide to measurement and data analysis, 319-332, 2012.

Mueller, B., Seneviratne, S.I.: Systematic land climate and evapotranspiration biases in CMIP5 simulations, Geophysic Research Letters, 41, 128–134, 2014.

Noilhan, J. and Planton, S.:. A simple parameterization of land surface processes for meteorological models, Mon. Wea. Rev., 117, 536-549, 1989.

Noilhan, J. and Mahfouf, J.-F.: The ISBA land surface parameterisation scheme, Global and Planetary Change, 13, 145-159, 1996.

Noilhan, J., Donier, S., Sarrat, C., Moigne, P. L.: Regional-scale evaluation of a land surface scheme from atmospheric boundary layer observations, J. Geophys. Res., 116, 1-17, 2011.

Olioso, A., Carlson, T.N., and Brisson, N.:Simulation of diurnal transpiration and photosynthesis of a water stressed soybean crop. Agric. For. Meteorol. 81, 41–59, 1996.

Olioso, A., Chauki, H., Courault, D., and Wigneron, J.-P.: Estimation of Evapotranspiration and Photosynthesis by Assimilation of Remote Sensing Data into SVAT Models, Remote Sensing of Environment, Volume 68, 341-356, 1999.

Olioso, A., Braud, I., Chanzy, A., Courault, D., Demarty, J., Kergoat, L., Lewan, E., Ottlé, C., Prévot, L., Zhao, W.., Calvet, J.-C., Cayrol, P., Jongshaao, R., Moulin, S., Noilhan, J., Wigneron, J.-P.: SVAT modeling over the Alpilles-ReSeDA experiment: comparing SVAT models over wheat fields, Agronomie 22, 651–668, 2002.

Olioso, A., Inoue, Y., Ortega-FARIAS, S., Demarty, J., Wigneron, J.-P., Braud, I., Jacob, F., Lecharpentier, P., Ottle, C., Calvet, J.-C., Brisson, N.: Future directions for advanced evapotranspiration modeling: Assimilation of remote sensing data into crop simulation models and SVAT models, Irrigation and Drainage Systems 19, 377–412, 2005.

Overgaard, J., Rosbjerg, D., Butts, M. B.: Land-surface modelling in hydrological perspective – a review, Biogeosciences, 3, 229-241, 2006.

Pitman, A. J.: The evolution of, and revolution in, land surface schemes designed for climate models, Int. J. Climatol., 23: 479–510. doi: 10.1002/joc.893, 2003.

Quintana-Seguí, P., Le Moigne, P., Durand, Y., Martin, E., Habets, F., Baillon, M., Canellas, C., Franchisteguy, L., Morel, S.: Analysis of Near-Surface Atmospheric Variables: Validation of the SAFRAN Analysis over France. Journal of Applied Meteorology and Climatology, 47, 92-107, 2008.

Rebmann, C., Kolle., O., Heinesch, B., Queck., R, Ibrom, A., Aubinet., M.: Data acquisition and flux calculation, in Aubinet, M., Vesala, T., Papale, D., (Eds), Eddy Covariance: A practical guide to measurement and data analysis, Springer, pp. 59-84, 2012.

Richardson, A.D., Hollinger, D.Y., Burba, G.G., Davis, K.J., Flanagan, L.B., Katul, G.G., William Munger, J., Ricciuto, D.M., Stoy, P.C., Suyker, A.E., Verma, S.B., Wofsy, S.C.: A multi-site analysis of random error in tower-based measurements of carbon and energy fluxes, Agr. Forest Meteorol., 136, 1–18, 2006.

Sellers, P. J., and Dorman, J. L.:: Testing the Simple Biosphere Model (SiB) Using Point Micrometeorological and Biophysical Data, J. Climate Appl. Meteor., 26, 622–651, 1987.

Schaap, M. G., Leij, F. J., and van Genuchten, M. T.: ROSETTA: a computer program for estimating soil hydraulic parameters with hierarchical pedotransfer functions, J. Hydrol., 251, 163– 176 , 2009.

Scharnagl, B., Vrugt, J. a., Vereecken, H., Herbst, M.: Inverse modelling of in situ soil water dynamics: investigating the effect of different prior distributions of the soil hydraulic parameters, Hydrol. Earth Syst. Sci., 15, 3043–3059, 2011.

Steenpass, C., Vanderborght, J., Herbst, M., Simonek, J., and Vereecken, H.: Estimating soil hydraulic properties from infrared measurements of soil surface temperatures and TDR data, Vadose Zone J., 9, 910–924,

Twine, T.E., Kustas, W.P., Norman, J.M., Cook, D.R., Houser, P.R., Meyers, T.P., Prueger, J.H., Starks, P.J., Wesely, M.L.: Correcting eddy-covariance flux underestimates over a grassland, Agr. Forest Meteorol., 103, 279–300, 2000.

Vereecken, H., Maes, J., and Darius, P.: Estimating the soil moisture retention characteristic from texture, bulk density and carbon content, Soil Sci., 148, 389–403, 1989.

Verhoef, A., Egea, G.,. Modeling plant transpiration under limited soil water: Comparison of different plant and soil hydraulic parameterizations and preliminary implications for their use in land surface models. Agric. For. Meteorol. 191, 22–32, 2014.

Vidal, J.-P., Martin, E., Franchistéguy, L., Habets, F., Soubeyroux, J.-M., Blanchard, M., and Baillon, M: Multilevel and multiscale drought reanalysis over France with the Safran-Isba-Modcou

hydrometeorological suite, Hydrol. Earth Syst. Sci., 14, 459-478, doi:10.5194/hess-14-459-2010, 2010.

Vrugt, J. a., Braak, C.J.F., Gupta, H. V., Robinson, B. a., 2008. Equifinality of formal (DREAM) and informal (GLUE) Bayesian approaches in hydrologic modeling ? Stoch. Environ. Res. Risk Assess. 23, 1011–1026.

Wetzel, P. J., and Chang, J. T.:Concerning the relationship between evapotranspiration and soil moisture, J. Climate Appl. Meteor., 26, 18–27, 1987.

Wilson, K., Goldstein, A., Falge, E., Aubinet, M., Baldocchi, D., Berbigier, P., Bernhofer, C., Ceulemans, R., Dolman, H., Field, C., Grelle, A., Ibrom, A., Law, B.E., Kowalski, A., Meyers, T., Moncrieff, J., Monson, R., Oechel, W., Tenhunen, J., Valentini, R., Verma, S.: Energy balance closure at FLUXNET sites, Agr. Forest Meteorol., 113, 223–243, 2002.

Workmann, S. R. and Skaggs, R. W.: Sensitivity of water management models to approaches for determining soil hydraulic properties, Transaction of the ASAE, 37(1), 95–102, 1994.

Tables

Table 1: 2001-2012 crop succession. The first sunflower in 2003 (1) was stopped and replaced by a new one. The 2009 maize (2) was stopped and replaced by sorghum because the emergence of maize was too heterogeneous. T and Rain are the mean temperature and cumulative precipitation, respectively, over the crop cycle.

Year	Crop	Sowing date	Harvest date	Irrigation (mm)	Rain (mm)	T (°C)
2001	Maize	2001/04/25	2001/09/28	375	232.0	20.7
2002	Wheat	2001/10/23	2002/07/02	0	399.0	11.6
2003	Sunflower[1]	2003/04/16	2003/05/26	40	68.0	17.1
2003	Sunflower	2003/06/02	2003/09/19	225	68.5	24.8
2004	Wheat	2003/11/07	2004/06/28	0	422.0	11.2
2005	Peas	2005/01/13	2005/06/22	100	203.5	11.9
2006	Wheat	2005/10/27	2006/06/27	20	256.0	10.7
2007	Sorghum	2007/05/10	2007/10/16	80	168.5	20.6
2008	Wheat	2007/11/13	2008/07/01	20	502.5	11.7
2009	Maize[2]	2009/04/23	2009/06/15	80	110.5	19.2
2009	Sorghum	2009/06/25	2009/09/22	245	89.0	23.6
2010	Wheat	2009/11/19	2010/07/13	0	446.5	11.6
2011	Sorghum	2011/04/22	2011/09/22	60	268.5	21.4
2012	Wheat	2011/10/19	2012/06/25	0	437.0	12.0

Table 2: Mean soil properties over the 0-1.2m soil profile. density is the soil bulk density. θ_s is the soil moisture at saturation derived from bulk density measurements. θ_{wp}, θ_{fc} are the soil moisture at wilting point and field capacity, respectively derived from laboratory methods for given hydraulic conductivity (K) or matric potential (h) levels. The second and third rows represent the vertical (σ_V) and the spatio-temporal (σ_{ST}) variability of these measurements, respectively.

	clay (%)	sand (%)	density (g cm^{-3})	θ_s ($m^3 m^{-3}$)	θ_{wp} (h=-150 m) ($m^3 m^{-3}$)	θ_{fc} (h=-3.3 m) ($m^3 m^{-3}$)	θ_{fc} (K=0.1 mm day^{-1}) ($m^3 m^{-3}$)
Mean	**33.15**	**13.95**	**1.57**	**0.390**	**0.170**	**0.344**	**0.268**
σ_V	0.58	1.14	0.16	0.056	0.011	0.021	0.027
σ_{ST}	na	na	0.05	0.019	na	na	na

Table 3: Estimates of the rooting depth ($Z_{root\text{-}zone}$), the soil moisture at field capacity (θ_{fc}) and the soil moisture at wilting point (θ_{wp}) derived from the time evolution of vertical profiles of field-measured soil moisture. MaxAWC (mm) represents the maximum root-zone water stock available for the crop. When no measurements were available, the mean value (*in italic*) from similar crop type was used. The last two rows are the mean and the SD computed over all crop cycles.

Crop	Year	$Z_{root\text{-}zone}$ (m)	θ_{fc} ($m^3\ m^{-3}$)	θ_{wp} ($m^3\ m^{-3}$)	MaxAWC (mm)
Maize	2001	1.45	0.320	0.174	212
Wheat	2002	1.55	0.314	0.126	291
Sunflower	2003	1.80	0.311	0.209	184
Wheat	2004	1.65	0.314	0.183	216
Peas	2005	1.00	0.308	0.218	90.0
Wheat	2006	1.85	0.309	0.179	241
Sorghum	2007	1.65	0.306	0.183	203
Wheat	2008	1.00	0.279	0.202	77.0
Maize	2009	*1.45*	*0.320*	*0.174*	*212*
Sorghum	2009	*1.65*	*0.306*	*0.183*	*203*
Wheat	2010	1.75	0.327	0.182	254
Sorghum	2011	*1.65*	*0.306*	*0.183*	*203*
Wheat	2012	*1.50*	*0.309*	*0.174*	*203*
mean		1.50	0.310	0.184	189
SD		0.30	0.012	0.025	56.0

Table 4: Values of the soil parameters used in the simulations. *PTF* corresponds to the standard implementation of the model achieved with the ECOCLIMAP-II rooting depth ($Z_{root-zone}$) and the pedotransfer estimates of the wilting point (θ_{wp}), the field capacity (θ_{fc}) and the saturation (θ_s). Distinct *in situ* estimates of these parameters are used in the other simulations. CV means time-variable values of $Z_{root-zone}$ and θ_{wp} retrieved over each crop cycle (see Table 3). MaxAWC is the maximum root-zone water stock available for the crop.

	Simulation cases			
Soil parameters	*PTF*	*LAB*	$FIELD_{cst}$	$FIELD_{var}$
θ_{sat} ($m^3\,m^{-3}$)	0.479	0.390	0.390	0.390
θ_{fc} ($m^3 m^{-3}$)	0.303	0.268	0.310	0.310
θ_{wp} ($m^3\,m^{-3}$)	0.214	0.170	0.184	CV
$Z_{root-zone}$ (m)	1.5	1.5	1.5	CV
MaxAWC (mm)	134	147	189	CV

Table 5: Performances of the simulated energy fluxes for the standard simulation *PTF*. RN is the net radiation. H, LE and G are the sensible, latent and ground heat fluxes. The metrics were computed over the valid measurements available for each variable. For LE, only the 2004-2012 period is used. N and r are the number of samples and the correlation coefficient, respectively.

RN (W m^{-2})				H (W m^{-2})				LE (W m^{-2})				G (W m^{-2})			
N	r	RMSE	BIAS	N	r	RMSE	BIAS	N	r	RMSE	BIAS	N	r	RMSE	BIAS
197255	0.99	27.7	0.2	103886	0.85	56.2	17.6	96214	0.80	52.4	-11.8	191619	0.88	46.9	-1.3

Table 6: Performances of simulated latent heat flux (LE), daily daytime evapotranspiration (ET_d) and root-zone soil moisture ($\theta_{root\text{-}zone}$) computed over the 20 November 2003-18 December 2012 period for which direct measurements of LE were available. ET_d was computed when 90% of daytime measurements were valid for each day. *PTF*, *LAB*, *$FIELD_{cst}$ and $FIELD_{var}$* are the simulations cases defined in Table 4. N is the number of samples used to evaluate each variable. Meas is the mean value of the measured variable.

	CROP CYCLE						**INTER-CROP**					
	LE (W m^{-2})		**ET_d** (mm day^{-1})		**$\theta_{root\text{-}zone}$ (m^3 m^{-3})**		**LE (W m^{-2})**		**ET_d** (mm day^{-1})		**$\theta_{root\text{-}zone}$ (m^3 m^{-3})**	
N	52260		944		179		43954		853		135	
Meas	70.1		1.64		0.255		35.6		0.85		0.247	
	RMSE	BIAS	RMSE	BIAS	RMSE	BIAS	RMSE	BIAS	RMSE	BIAS	RMSE	BIAS
PTF	61.6	-14.3	1.07	-0.30	0.034	0.022	38.6	-8.9	0.58	-0.17	0.033	0.026
LAB	60.7	-11.8	1.03	-0.24	0.030	-0.015	37.7	-7.6	0.55	-0.14	0.024	-0.011
$FIELD_{cst}$	61.8	- 0.3	1.00	0.07	0.024	0.012	40.7	-0.2	0.60	0.06	0.026	0.017
$FIELD_{var}$	61.3	1.0	1.00	0.10	0.022	0.012	38.8	-1.2	0.55	0.04	0.029	0.021

Table 7: Comparison of the direct measurement of LE (Direct), the energy balance residue estimate of LE (Residue) and the bowen ratio estimate of LE (Bowen). RMSD is the root mean square of the differences between the LE estimates. SDD is the SD of the differences between the LE estimates. For Y versus X, MD is computed as Y-X. In the last row, the MD in cumulative ET over 12-yr is computed relatively to X.

	Bowen versus Direct	Residue versus Direct	Bowen versus Residue
RMSD ($W\ m^{-2}$)	25.0	36.3	29.3
SDD ($W\ m^{-2}$)	23.9	36.2	28.9
MD ($W\ m^{-2}$)	7.5	3.2	4.3
MD over 12-years (mm)	727	310	417
MD over 12-years (%)	12	5	6.5

Table 8: Mean and SD of the parameters used in the Monte-Carlo analysis. g_m C3 and g_m C4 denote the mesophyll conductance for C3 and C4 crop. The mean values are those used in the simulation *FIELD$_{cst}$*.

	$Z_{root\text{-}zone}$ (m)	θ_{sat} ($m^3\ m^{-3}$)	θ_{fc} ($m^3\ m^{-3}$)	θ_{wp} ($m^3\ m^{-3}$)	g_m C3 m s^{-1}	g_m C4 m s^{-1}
mean	1.5	0.390	0.310	.184	0.001	0.009
SD	0.3	0.019	0.012	0.025	0.0007	0.007

Figures:

Figure 1: Map of the field site and locations of the instruments. Image from Google Earth, 2015.

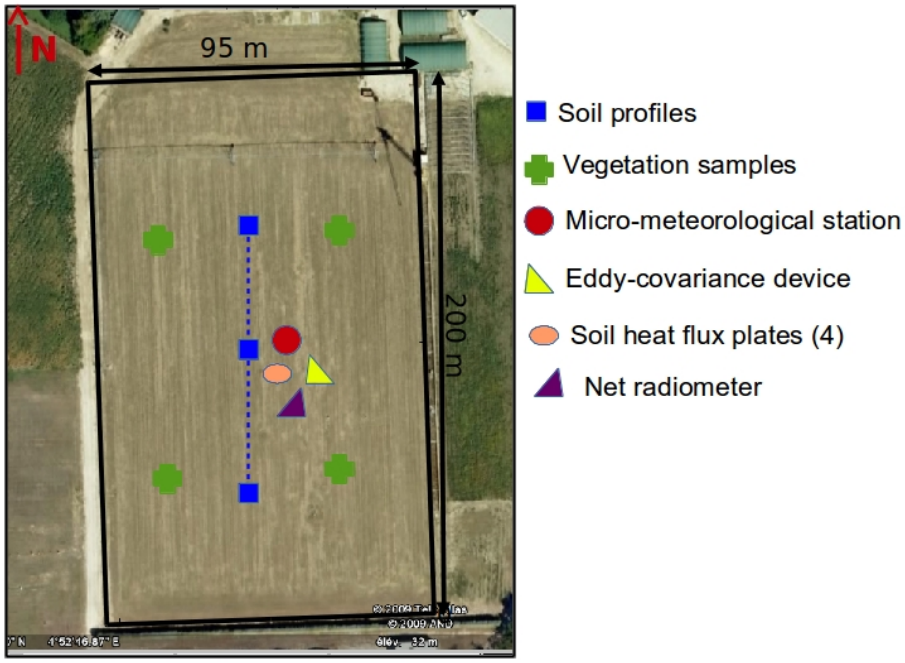

Figure 2: Illustration of the typical succession of winter and summer crop over the Avignon site and implementation of the crop succession in the simulations. Θ and T represent soil moisture and soil temperature transmitted from one sub-simulation to the following one.

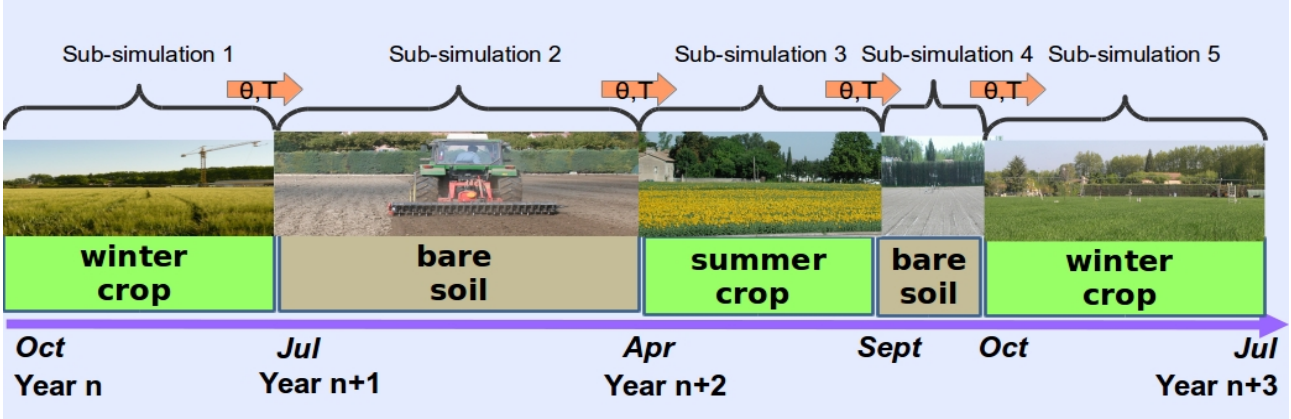

Figure 3.: Evolution of simulated and measured evapotranspiration (ET in mm), simulated soil evaporation (E in mm), simulated plant transpiration (T in mm), simulated and measured daily daytime ET (ET_d in mm), simulated and measured daily mean of root-zone soil moisture ($\theta_{root\text{-}zone}$ in m^3 m^{-3}), 10-d rainfall plus irrigation (in mm), daily mean of *in situ* Leaf Area Index (LAI in m^2 m-2) over the 2001-2012 period. For clarity reasons, the average of daily values over 10 days are displayed. Cumulative values were computed over the time steps for which valid ET measurements were available. ET_d was computed when 90% of valid daytime measurements were available for each day. The simulation corresponds to the standard implementation of the model (*PTF*). Crop and inter-crop periods are represented by grey and white background, respectively.

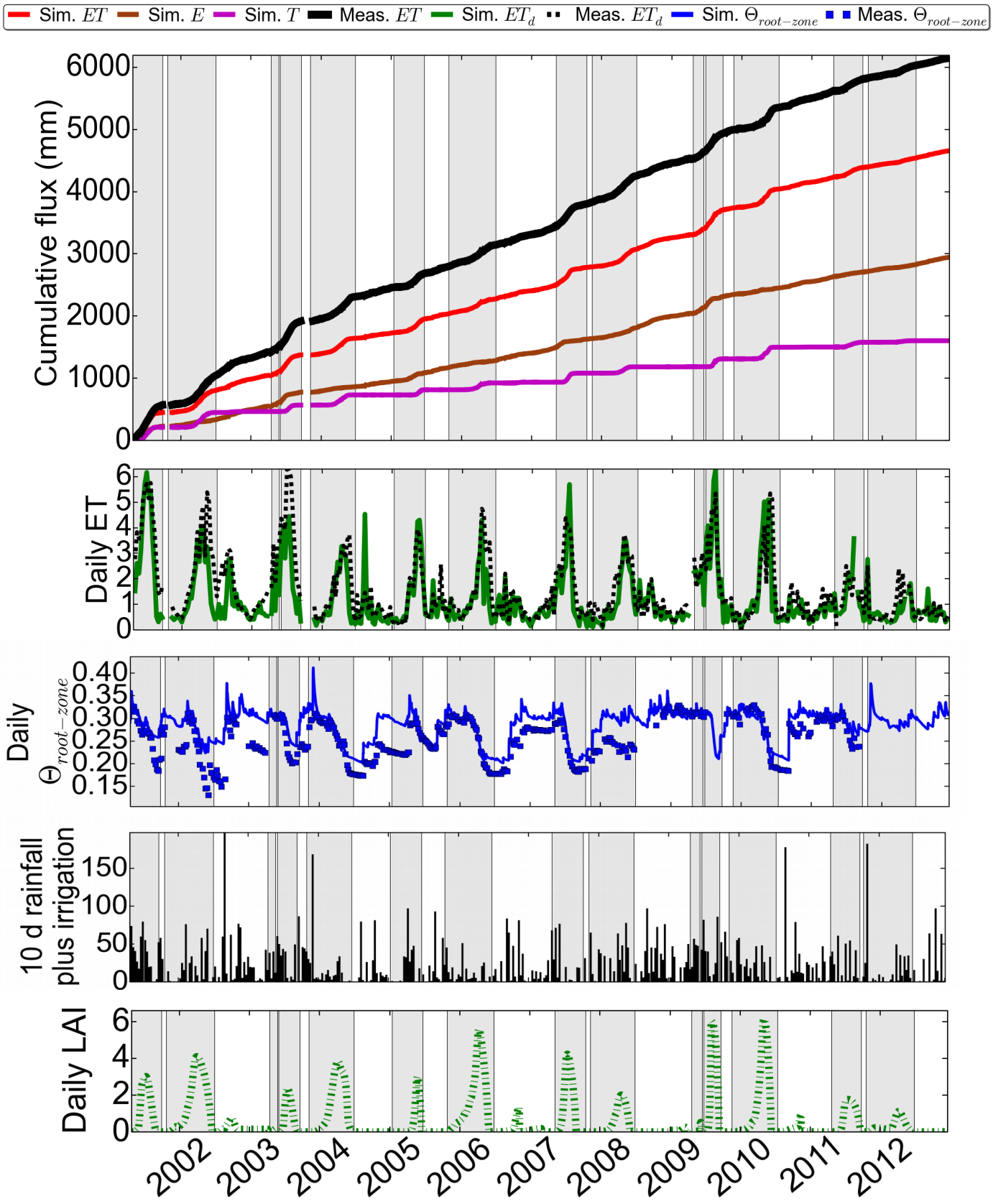
Sim. ET
Sim. E
Sim. T
Meas. ET
Sim. ET_d
Meas. ET_d
Sim. $\Theta_{root-zone}$
Meas. $\Theta_{root-zone}$
Cumulative flux (mm)
6000
5000
4000
3000
2000
1000
0
Daily ET
6
5
4
3
2
1
0
Daily $\Theta_{root-zone}$
0.40
0.35
0.30
0.25
0.20
0.15
10 d rainfall plus irrigation
150
100
50
0
Daily LAI
6
4
2
0
2002
2003
2004
2005
2006
2007
2008
2009
2010
2011
2012

1190

Figure 4: Sensitivity analysis: Impact of variations in soil moisture at saturation (θ_s), soil moisture at field capacity (θ_{fc}) and soil moisture at wilting point (θ_{wp}) on simulated (a) evapotranspiration (ET) and (b) soil evaporation (E) and plant transpiration (T), cumulated over the 12 year period. We display the difference in cumulative flux between the simulation PTF and the simulation PTF with modified soil parameter. FIELD means that the in situ values of the soil parameters (0.390, 0.310, 0.184 for θ_s, θ_{fc}, θ_{wp} respectively) are tested one by one.

(a)

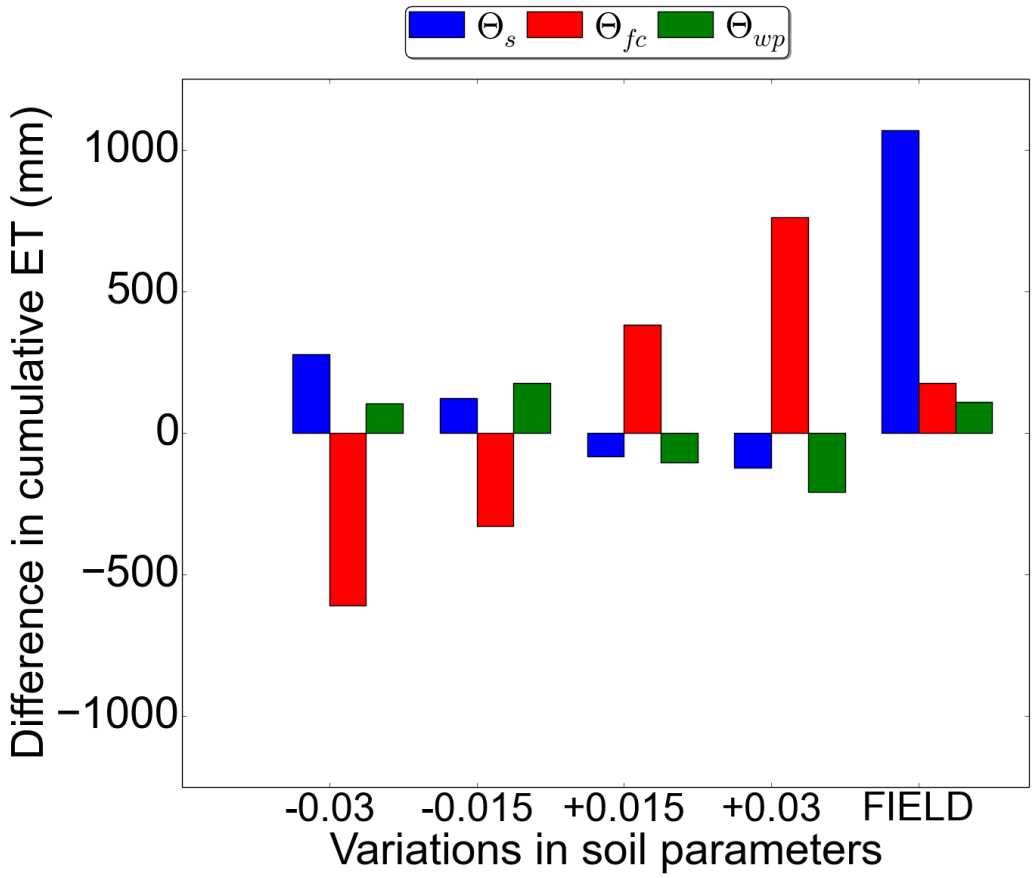

(b)

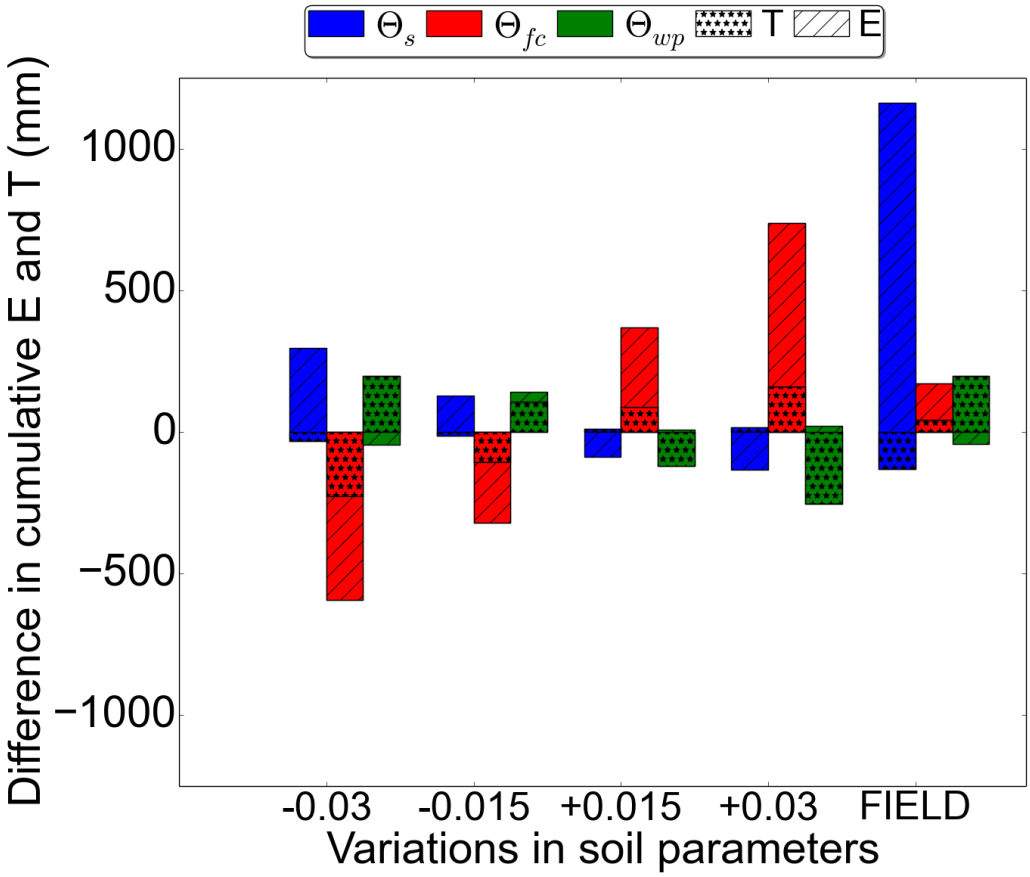
Θ_s
Θ_{fc}
Θ_{wp}
T
E
Difference in cumulative E and T (mm)
1000
500
0
−500
−1000
-0.03
-0.015
+0.015
+0.03
FIELD
Variations in soil parameters

Figure 5: Evolution of (a) measured and simulated evapotranspiration (ET) and (b) measured and simulated root-zone soil moisture ($\theta_{root\text{-}zone}$), over the wheat cycle in 2006. In panel a, the simulated transpirations (T) are represented by dashed lines and ET by solid lines. The LAI cycle is represented by green dash-dot lines. In panel b, Meas (1.50m) is the measured soil moisture integrated between 0 and 1.50 m and is used to evaluate the *PTF* and $FIELD_{cst}$ $\theta_{root\text{-}zone}$ which are simulated with Z_{root_zone}=1.5 m. Meas (1.85 m) is the measured soil moisture integrated between 0 and 1.85 m and is used to evaluate $FIELD_{var}$ $\theta_{root\text{-}zone}$ achieved with Z_{root_zone}=1.85 m for wheat crop in 2006.

a)

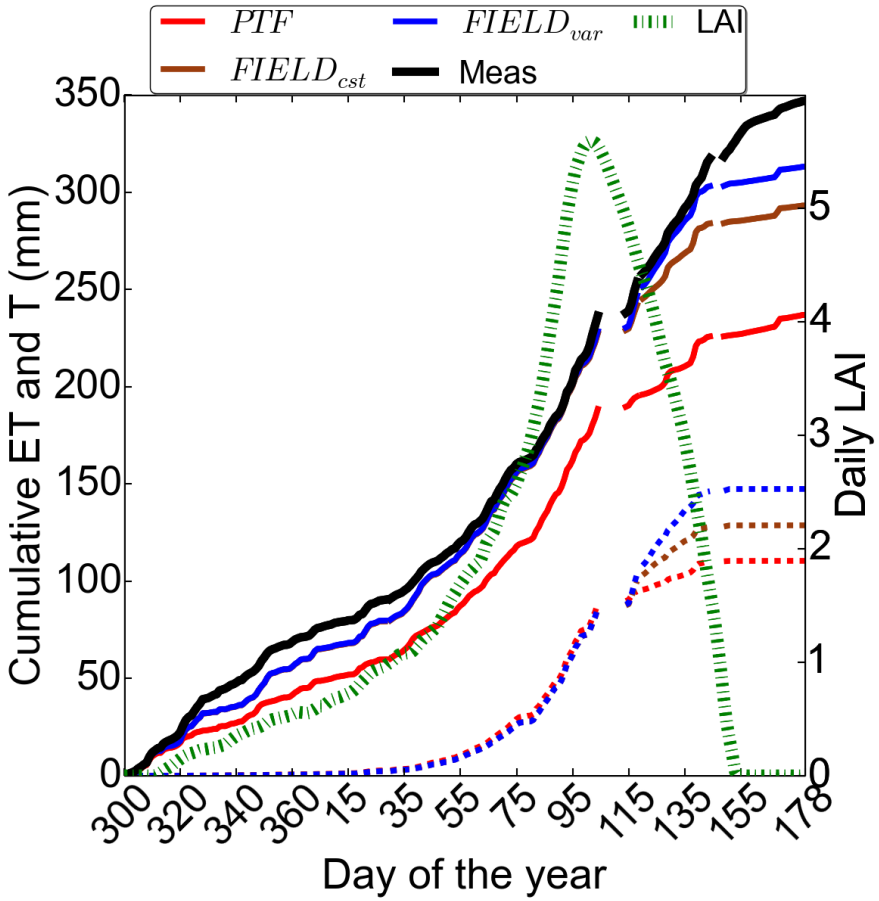

b)

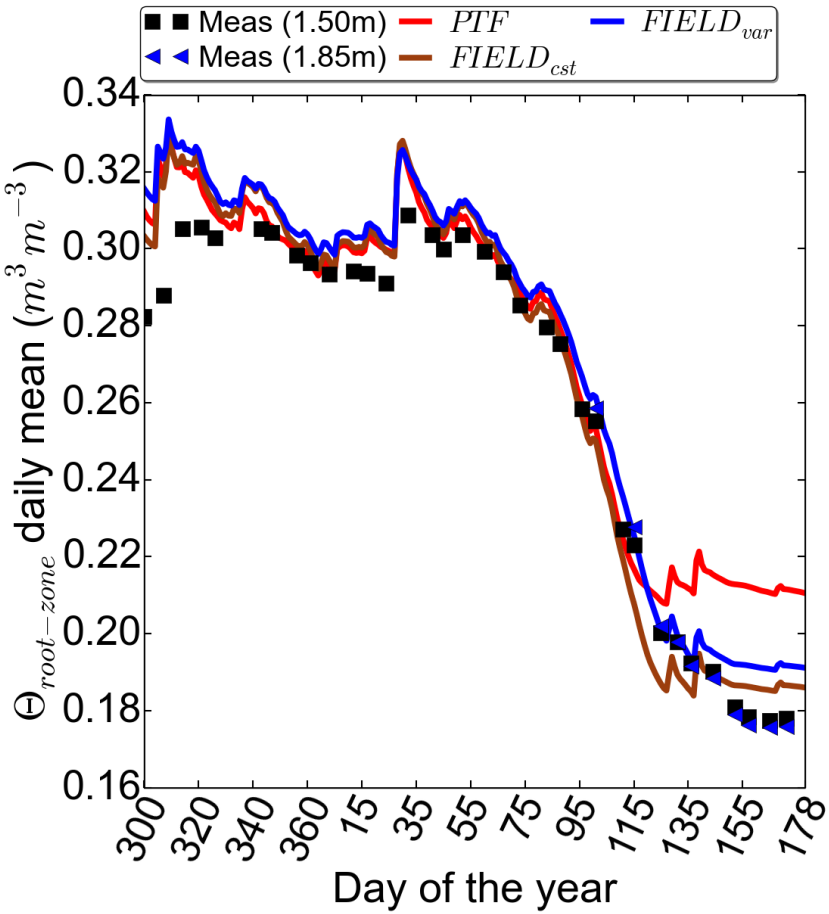

Figure 6: Evolution of (a) measured and simulated evapotranspiration (ET) and (b) measured and simulated root-zone soil moisture ($\theta_{root\text{-}zone}$), over the irrigated maize in 2001. In panel a, the simulated transpirations (T) are represented by dashed lines and ET by solid lines. The LAI cycle is represented by green dash-dot lines.

a)

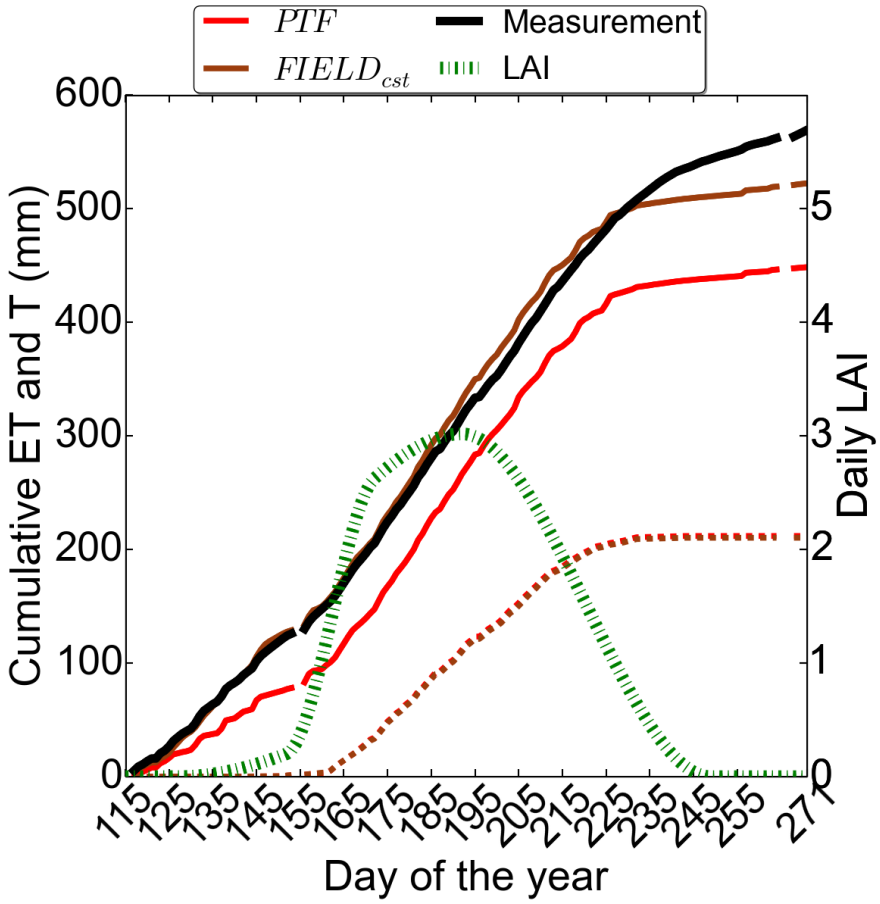

b)

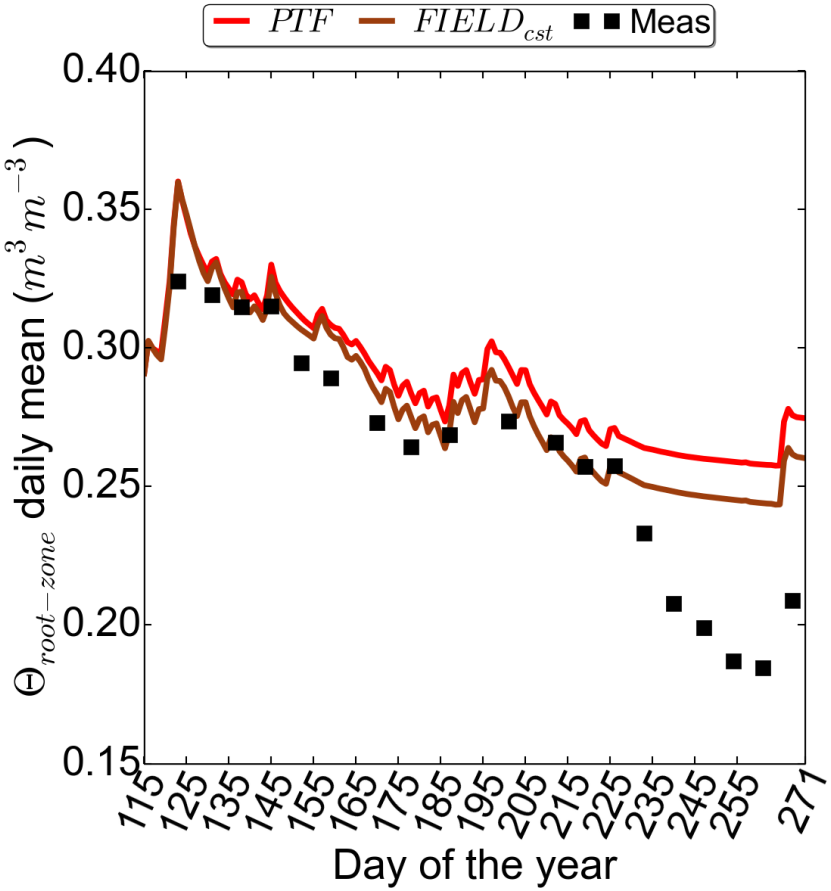

1245

Figure 7: Evolution of (a) measured and simulated evapotranspiration (ET) and (b) measured and simulated root-zone soil moisture ($\theta_{root\text{-}zone}$), over the inter-crop period in 2010. ET corresponds to the soil evaporation since the soil is bare.

a)

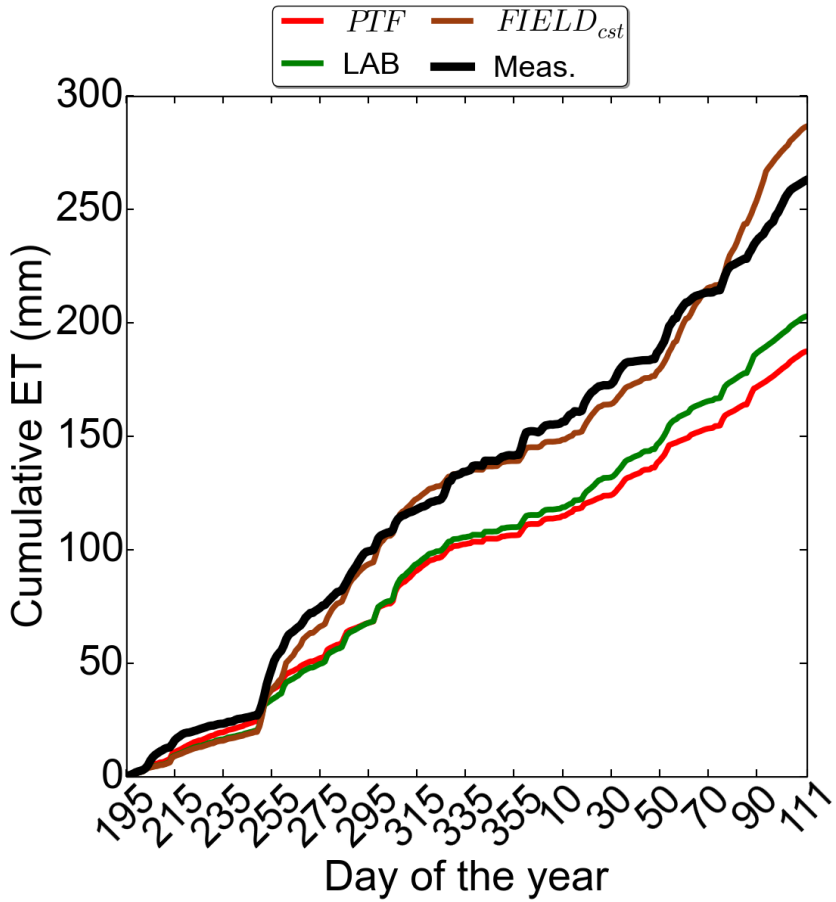

b)

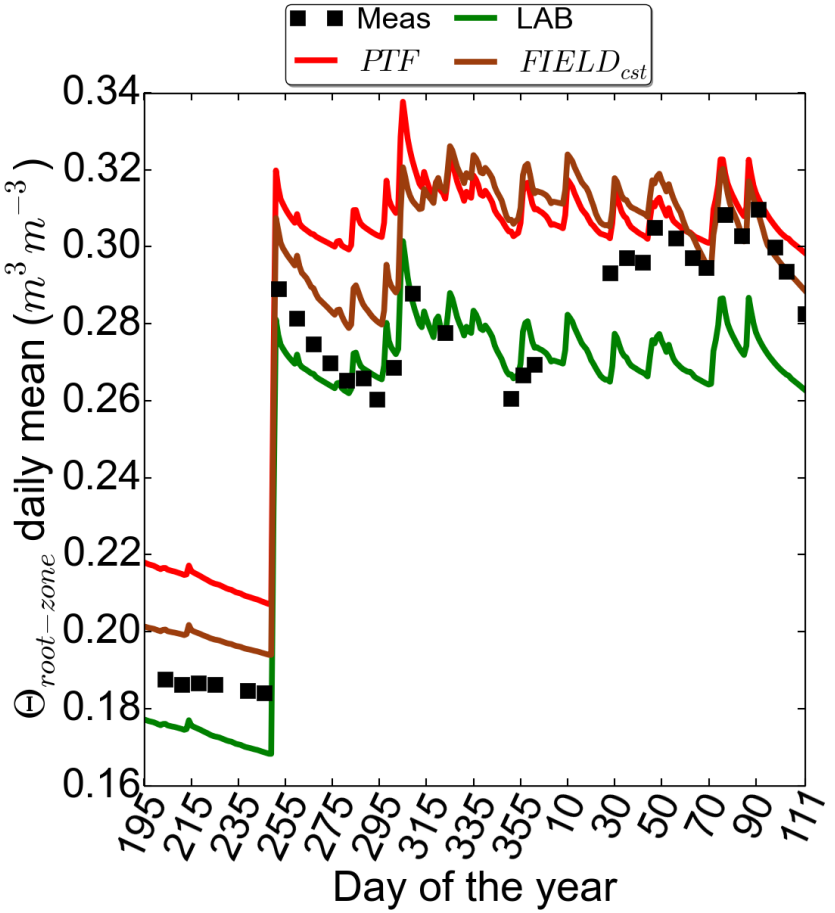

1250

Fig. 8: Propagation of the uncertainties in (a) the soil parameters ($Z_{root\text{-}zone}$, θ_s , θ_{fc} , θ_{wp}) and (b) the mesophyll conductance, on simulated ET. $FIELD_{cst}$ is the simulation achieved with the mean values of $Z_{root\text{-}zone}$, θ_s , θ_{fc} , θ_{wp} derived from the field measurements of soil moisture and the standard value of gm (Gibelin et al., 2006). The grey curves represent the 100 simulations generated by Monte-Carlo (MC). The 95% percentile interval (PI) of the MC simulations are computed over the empirical distributions of cumulative ET values.

(a)

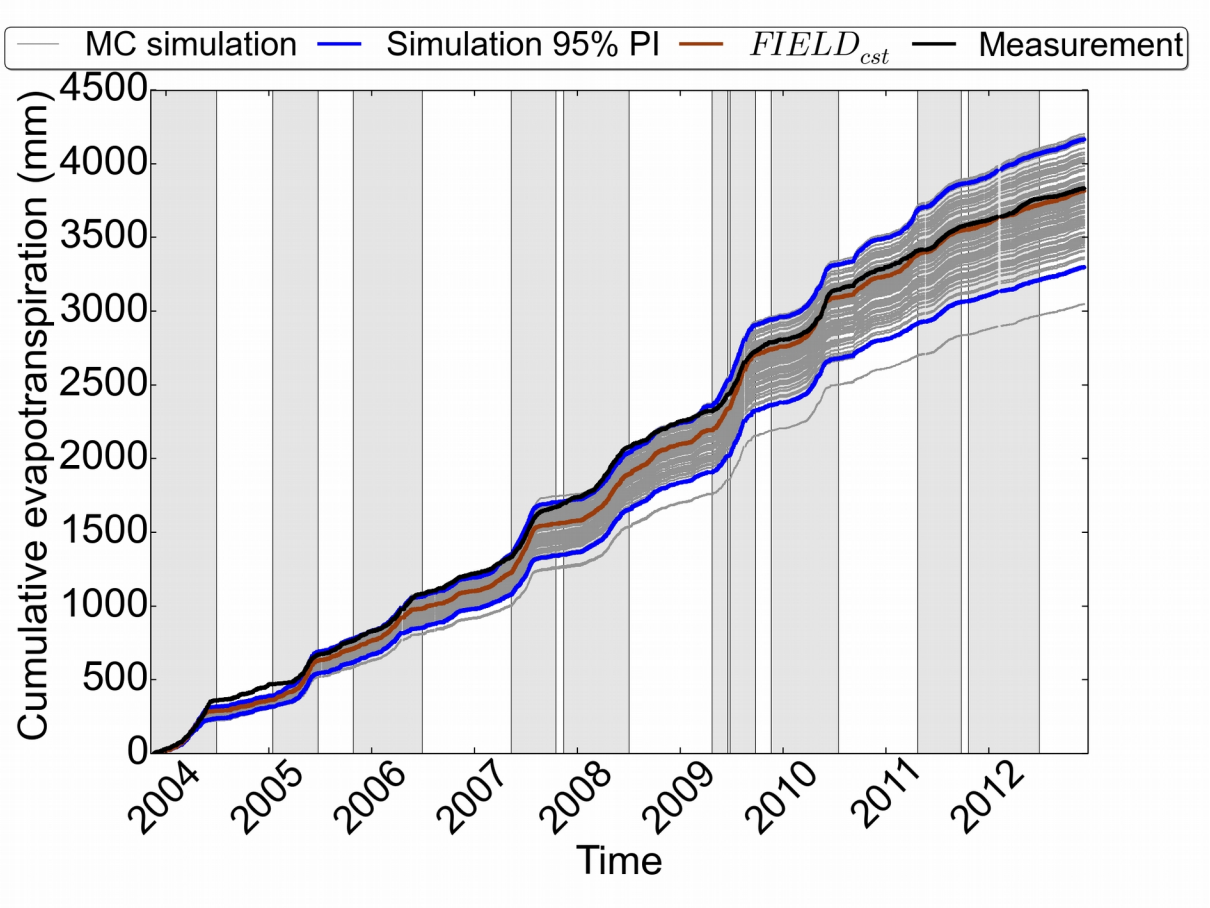
MC simulation
Simulation 95% PI
$FIELD_{cst}$
Measurement
Cumulative evapotranspiration (mm)
4500
4000
3500
3000
2500
2000
1500
1000
500
0
2004
2005
2006
2007
2008
2009
2010
2011
2012
Time

1285

(b)

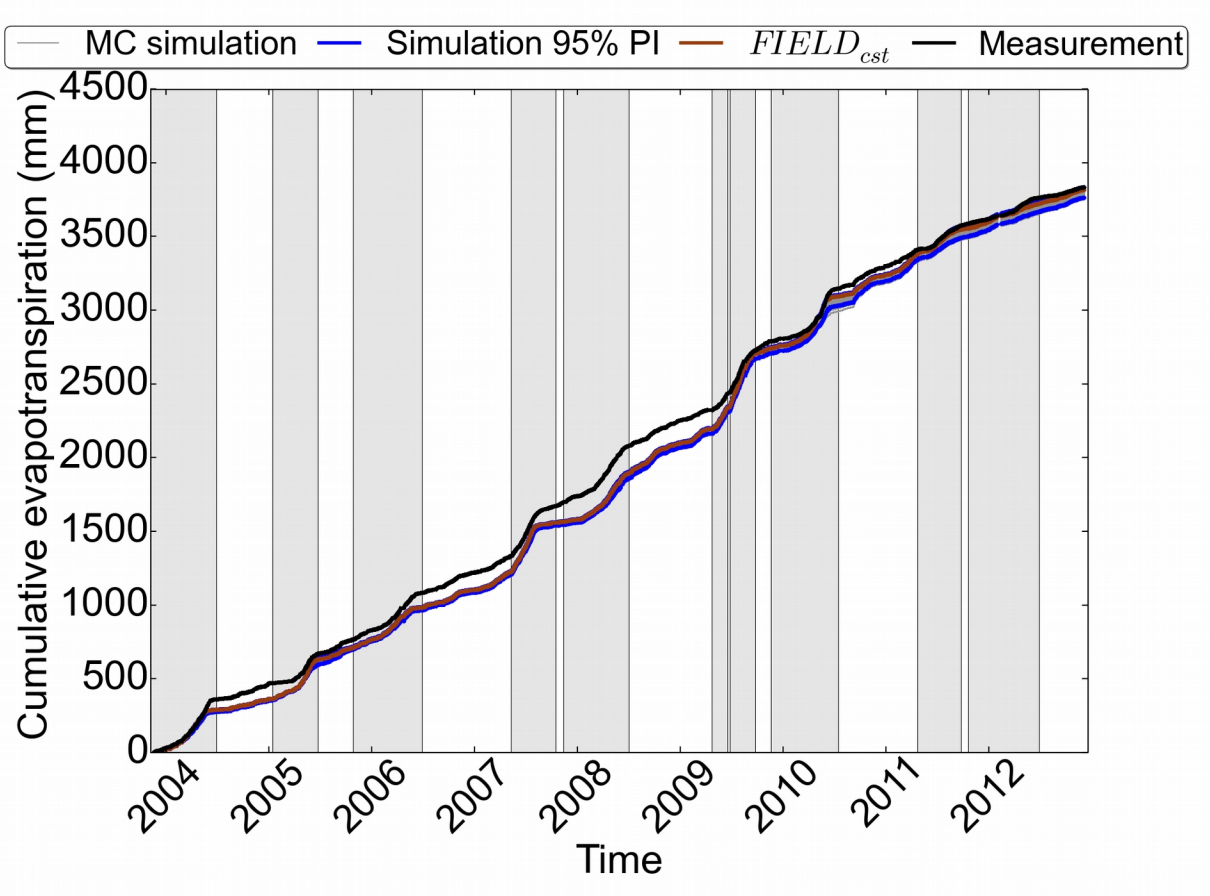
MC simulation
Simulation 95% PI
$FIELD_{cst}$
Measurement
Cumulative evapotranspiration (mm)
0
500
1000
1500
2000
2500
3000
3500
4000
4500
2004
2005
2006
2007
2008
2009
2010
2011
2012
Time

1295